Journal of Fluorescence, Vol. 15, No. 3, May 2005 (© 2005)
DOI: 10.1007/s10895-005-2632-1

Pitfalls and Their Remedies in Time-Resolved Fluorescence Spectroscopy and Microscopy

Martin vandeVen,[1] Marcel Ameloot,[1] Bernard Valeur,[2,3] and Noël Boens[4,5]

Received June 30, 2004; accepted January 11, 2005

Time-resolved fluorescence spectroscopy and microscopy in both time and frequency domains provide very useful and accurate information on dynamic processes. Good quality data are essential in obtaining reliable parameter estimates. Distortions of the fluorescence response due to artifacts may have disastrous consequences. We provide here a concise overview of potential difficulties encountered under daily laboratory circumstances in the use of time- and frequency-domain equipment as well as practical remedies against common error conditions, elucidated with several graphs to aid the researcher in visual inspection and quality-control of collected data. A range of artifacts due to sample preparation or to optical and electronic pitfalls are discussed, as are remedies against them. Also recommended data analysis strategies are described.

KEY WORDS: Time-resolved fluorescence spectroscopy; time-resolved fluorescence microscopy; artifacts; pulse fluorometry; phase-modulation fluorometry; FLIM; single-photon timing; sample preparation; optics; electronics; data analysis.

INTRODUCTION

Scope of This Contribution

The ability of fluorescence to provide temporal information is of the utmost importance in understanding photophysical, photochemical, and photobiological processes. Since the first determination of an excited-state lifetime by Gaviola [1], extraordinary progress has been made in both pulse and phase-modulation fluorometries. The use of high repetition rate (sub)picosecond lasers, microchannel plate (MCP) photodetectors, and sophisticated data analysis software (global analysis software for frequency and time domain: http://www.lfd.uiuc.edu/globals) have increased the time resolution up to a few picoseconds [2]. However, reliable time-resolved fluorescence measurements are difficult to carry out for many reasons, discussed later. The aim of this contribution is to give the reader insight into the many pitfalls that await the experimentalist. Since good quality data are essential in obtaining reliable decay parameter estimates, it is necessary to know how to avoid or to solve these problems. *It is preferable, as much as possible, to eliminate experimental distortions by experimental techniques rather than to correct them in data analysis*. Because of the disastrous effects that these distortions can have on the final result, we describe the main error sources and the methods to eliminate or reduce them. Although many of the described artifacts also occur in steady-state fluorometry, the focus of this contribution is on *time-resolved* fluorometric techniques. For time-domain measurements, only instrumentation where lasers are used as excitation source will be covered, because lasers are better capable of reliably generating trains of very short light pulses. For frequency-domain experiments, lamp and Light Emitting Diode (LED) continue

[1] Biomedisch Onderzoeksinstituut, Limburgs Universitair Centrum, School of Life Sciences, Transnationale Universiteit Limburg, 3590 Diepenbeek, Belgium.
[2] CNRS UMR 8531, Laboratoire de Chimie générale, CNAM, 292 rue Saint-Martin, 75141 Paris cedex 03, France.
[3] CNRS UMR 8531, Laboratoire PPSM, ENS-Cachan, 61 avenue du Président Wilson, 94235 Cachan cedex, France.
[4] Department of Chemistry, Katholieke Universiteit Leuven, Celestijnenlaan 200 F, 3001 Heverlee, Belgium.
[5] To whom correspondence should be addressed. E-mail: noel.boens@chem.kuleuven.be

to be valuable alternatives to laser and synchrotron light sources [3,4].

Trends and Advantages: From Cuvette-Based to Microscopy Techniques

The past decade has seen a marked shift from cuvette-based techniques to microscopy methods. Cuvette-based experiments are very useful for obtaining spectral and temporal information on the ensemble averaged properties of cellular suspensions and well-controlled molecular solutions. With microscopy methods, knowledge about the statistical variation in properties of minute quantities and even single molecule both in time (time series) as well as in 2D and 3D space (z-stacks) can be obtained. Indeed, fluorescence microscopy in confocal configuration and/or with two-photon excitation has the advantage of three-dimensional spatial resolution. Very small excitation volumes (femtoliter range) are possible, so that a greatly reduced amount of material is required. Living cells and tissues can be studied with respect to their spatial and temporal variations.

A wide range of techniques has been implemented allowing almost nondestructive microscopic observation of real-time interactions between molecules in biochemical processes in living cells. Discrimination in emission wavelength, intensity, and polarization has helped to understand and elucidate numerous complex cellular interactions related to local changes in pH, ion concentrations, and membrane potential. However, many interactions may go undetected because light scatter and background fluorescence interfere with the detection of the often weak signals of interest. Further, variations in fluorescence intensity in a cell do not necessarily mean local differences in concentration because they can be caused by local variations in quantum yield and quenching effects. In microscopic or macroscopic imaging measurements, contrast can be enhanced independent of fluorophore concentration by fluorescence lifetime and time-resolved anisotropy measurements. Fluorescent lifetime imaging (FLIM) can map the cellular microenvironments through the changes in fluorescence decay time of the fluorophores. A brief overview is provided in reference [5]. Image contrast is further enhanced by the application of Förster resonance energy transfer (FLIM-FRET) [6] for studying molecular closeness on a nm scale and by total internal reflection fluorescence measurements (TIRF-FLIM) [7,8] for studying surface and interface phenomena.

Two General Methods: SPT (TCSPC) and MPF

Two time-resolved techniques are commonly used to record the time profile of the emitted fluorescence: one in the time domain (pulse fluorometry) and one in the frequency domain (phase-modulation fluorometry) [2,9]. The Single-Photon Timing (SPT) technique [10,11]—also called Time-Correlated Single-Photon Counting (TCSPC)—uses very short optical exciting pulses to obtain the sample fluorescence decay (a convolution of the instrument response function with the fluorescence δ-response of the sample). Figure 1 shows a schematic overview of a SPT set-up. In phase-modulation fluorometry, a frequency-domain method, also a Continuous Wave (CW) light source can be used by delivering a sinusoidal modulated excitation of variable frequency. Using a set of modulation frequencies ranging from a few to hundreds of MHz the time-resolved fluorescence response of the sample is obtained in the so-called multi-frequency phase-modulation fluorometry (MPF). Figure 2 shows a block diagram of a MPF set-up. Pulse fluorometry and phase-modulation fluorometry give in principle equivalent results coupled as they are by a Fourier transform [12]. Optical pulse trains can therefore also be used in MPF. The latest generations of instruments both use lasers and microchannel plate (MCP) detectors (for timing characteristics of detectors: http//ww.becker-hickl.de/pdf/spcdetect1.pdf). The time resolution of a phase-modulation fluorometer using the harmonic content of a mode-locked picoseconds laser and a MCP photomultiplier is comparable to that of a SPT instrument using the same kind of excitation source and detector. The SPT technique offers several advantages: high sensitivity, outstanding dynamic range and linearity (several decades of decay can be followed), well-defined statistics allowing proper weighting of each data point in data analysis, visualization of the fluorescence decay, recording of time-resolved spectra is easier than in phase-modulation fluorometry. The phase-modulation fluorometry has its own benefits: lifetime-based decomposition of spectra into their constituting components is simpler than in pulse fluometry. The data collection is generally faster particularly if a small number of frequencies is used. The short acquisition time for phase shift and modulation ratio measurements at a given frequency is a distinct advantage in fluorescence lifetime-imaging (FLIM). To summarize, pulse and phase-modulation fluorometries are rather complementary instead of competitive methods [2,13]. This view is pointedly shown in a unifying graphical form in reference [14]. Examples of time- and frequency-domain FLIM setups are presented in Figs. 3 and 4.

The principle of operation for a heterodyning cross-correlation MPF is displayed in Fig. 5. Theory has been described many times over (see e.g., reference [9]). In brief, sinusoidal intensity-modulated excitation light with angular frequency $\omega = 2\pi f$ excites a fluorophore. The

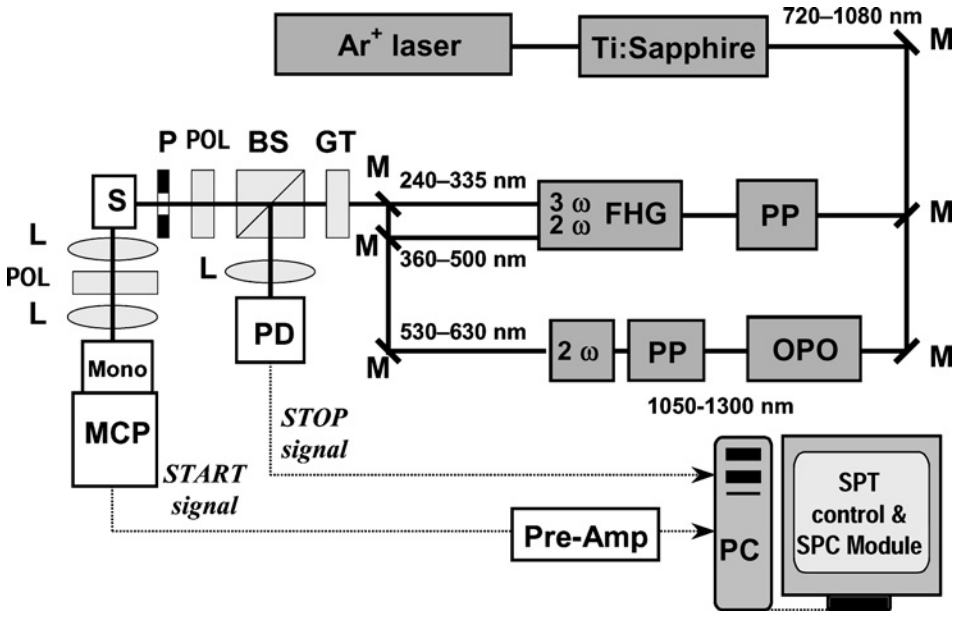

Fig. 1. Schematic overview of SPT set-up. BS: beam splitter, FHG: frequency harmonic generator, GT: Glan Thomson polarizer, L: lens, M: mirror, MCP: microchannel plate photomultiplier, Mono: monochromator, OPO: optical parametric oscillator, P: pinhole, PC: personal computer, PD: photodiode, POL: polarizer, PP: pulse picker, Pre-Amp: rise-time preamplifier, S: sample (compartment), SPC module: contains constant fraction discriminator, time-to-amplitude converter and multi-channel analyzer. The available wavelengths are also indicated.

fluorescence emission possesses the same modulation frequency but it is delayed in time and smaller in amplitude. The phase shift, $\Delta\varphi$, and demodulation, M, are related to the lifetime, τ, of the fluorescent excited state by

$$\Delta\varphi = \tan^{-1}(\omega\tau) \tag{1}$$

$$M = M_{\mathrm{M}}/M_{\mathrm{X}} = (1 + (\omega\tau)^2)^{-1/2} \tag{2}$$

where M_{X} and M_{M} are the modulation of excitation and emission, respectively. For a range of frequencies, phase difference and demodulation are measured. For a monoexponential decay the lifetime calculated from the phase data, τ_φ, and the one obtained from the modulation values, τ_{M}, has to be equal for all frequencies. This constitutes an easy way to quickly check instrument performance for a fluorescent lifetime standard with known single-exponential decay under well-controlled experimental conditions. In the case of a multiexponential decay or a distribution of decay times, we have $\tau_\varphi < \tau_{\mathrm{M}}$, but τ_φ can be greater than τ_{M} for a difference of exponentials as a result of an excited-state process. Now τ_φ and τ_{M} denote mean decay times. Determination of phase difference and demodulation for a set of at least 8 or 10 and better 20–30 frequencies, and application of a nonlinear least-squares fitting program allows precise decay time determination. In practice to eliminate artifacts a differential measurement is made by the alternating measurement of a sample against a reference fluorophore until a given preset accuracy is reached. Typically the standard deviations are 0.1–0.2° for the phase and 0.002–0.004 for the modulation.

A concise overview with principles of operation and instrument layouts for time- and frequency-domain FLIM is provided in reference [2]. In brief, the heart of a typical FLIM instrument is the detector assembly. It can consist of a gated intensifier–MCP [15] with an imaging detection CCD camera. In the time domain the gating configuration allows image acquisition in narrow time windows each with a variable delay sampling the spatial and temporal fluorescence decay characteristics. Frequency-domain phase fluorometry uses a similar detector gate configuration but now driven with a sine-wave modulation signal. The technique comes in two flavors. The modulation signal can have exactly the same frequency as the excitation optical signal, homodyne = phase-sensitive detection. High frequency information is converted to a DC signal [16]. The response for a set of chosen phase angle lags at each selected frequency is determined. When the detector modulation is offset by a small difference (beat) frequency with respect to the excitation, heterodyne or cross-correlation detection takes place for a series of chosen frequencies. The limiting factor is the phosphor

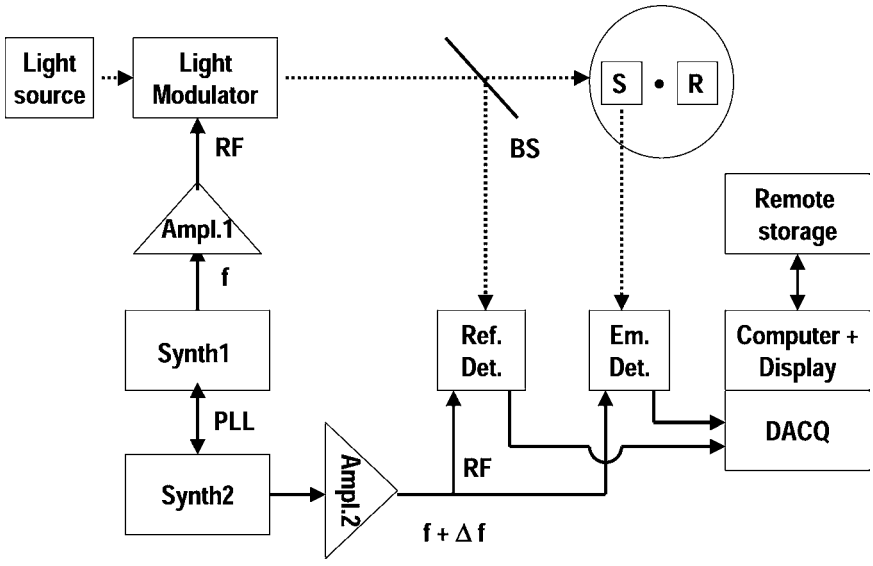

Fig. 2. Block diagram of a heterodyning multifrequency phase modulation fluorometer (MPF) for lamp and CW laser excitation. Two computer controlled frequency generators (Synth1 and Synth2) are connected through a phase-locked-loop (PLL). One synthesizer signal drives after amplification via radiofrequency (RF) amplifier Ampl. 1 the Pockels cell or AOM Light Modulator at frequency *f*. A second synthesizer (Synth2) signal modulates after amplification (Ampl.2) the detector gains at a frequency $f + \Delta f$. A reference detector (Ref. Det.) records the light source phase and modulation via a beam splitter (BS). An emission detector (Em. Det.) samples the phase shift and demodulation of the emitted fluorescence or scatter signal. For each frequency a two-position turret alternates between sample (S) and reference (R) cuvette positions until preset phase and modulation errors or maximum measurement time are reached. Fast Fourier Transform digital acquisition (DACQ) filters the heterodyne or cross-correlation frequency, Δf. In case a pulsed lightsource is used, its driving synthesizer is phase-locked to the detector synthesizer. In case a homodyning MPF is used both lightsource and detector synthesizer operate at the same frequency *f*. A phase shifter steps through the detector signal phases.

retention time of the photocathode phosphor. The faster the phosphor decay the higher the heterodyne frequency difference can be chosen. An alternative configuration uses a scanning one- or multiphoton laser beam accompanied by nonimaging cooled PMT detection. Recent FLIM overviews review both time- and frequency-domain implementations [6,17]. SPT FLIM methods have been aided by the commercial availability of single-card computer boards for nonimaging detection that can be readily interfaced to existing laser scanning microscopes in descanning or nondescanned modes.

Aims and Preview

This review aims at giving the researcher a good understanding of the many pitfalls in time-resolved fluorometry and microscopy, and indicates how they can be avoided or remedied. Both time and frequency-domain techniques are covered. For checking time-resolved instrument performance a standard calibration procedure should be followed at all times. To this end well-characterized single-fluorescence decay fluorophores with accurately described experimental conditions should be used [2,18]. In comparing old data with results obtained with the latest technologies, it becomes strikingly clear that over time the number of so-called reliable single-lifetime fluorophores has decreased dramatically from several hundred to about a few tens of fluorophores. This is mostly because of the ever-increasing instrumentation accuracy, sensitivity and reliability. For obtaining reliable optimum results during these lifetime and anisotropy tests, a concise description is presented of artifacts and effects due to sample preparation, optical, electronic pitfalls and remedies against them, as well as recommended data analysis strategies to be pursued.

First, we discuss artifacts related to sample preparation. This is followed by an overview of observed optical and electronic pitfalls. Proper data analysis strategies certainly are equally important and will be treated. Since

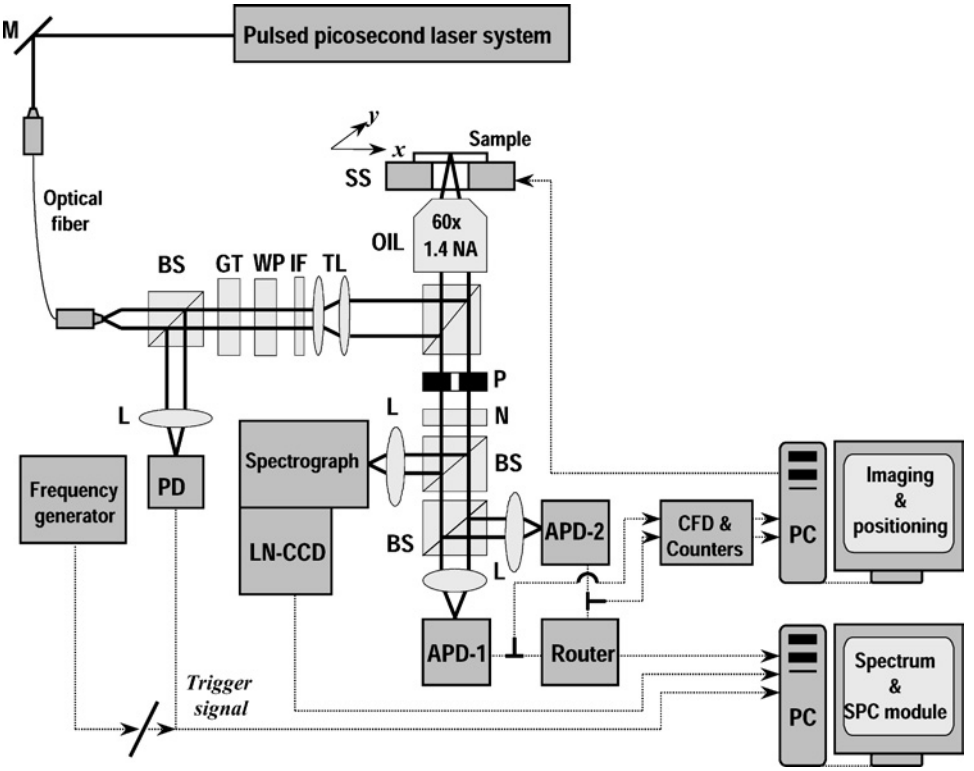

Fig. 3. Schematic diagram of confocal epi-illuminated fluorescence microscope set-up. APD: avalanche photodiode, BS: nonpolarizing beam splitter, CFD: constant fraction discriminator, GT: Glan Thomson polarizer, IF: interference band pass filter, L: lens, LN-CCD: liquid nitrogen cooled charge coupled device camera, M: mirror, N: notch filter, NA: numerical aperture, OIL: oil-immersion objective lens, P: pinhole, PC: personal computer, PD: photodiode, SPC module: contains constant fraction discriminator, time-to-amplitude converter and multichannel analyzer, SS: feedback-controlled *x*–*y* scanning stage, TL: telescopic lens system, WP: wave plate.

the lifespan of typical instrumentation may surpass 10–15 years, previous and older technologies will be considered as far as relevant to the current overview.

ARTIFACTS RELATED TO SAMPLE PREPARATION

Pitfalls and remedies in fluorescence measurements are generally applicable not only to fluorescence lifetime and anisotropy determination but also to steady-state experiments. Several experimental conditions have been described in the literature [19,20] but generally the information is disperse and cannot be easily located. Many trouble-causing phenomena can easily be prevented by proper preparation procedures. Some effects, however, are subtle and may be appreciated only after spending considerable time and effort in locating the error source and implementing a remedy.

Molecular oxygen (O_2) is a well-known quencher of fluorescence, but its effect on decay times (and quantum yields) strongly depends on the nature of the compound and the medium. The contribution of oxygen quenching to the decay of an excited state can be expressed by an additional quenching term. The concentration of atmospheric oxygen in most solvents is 10^{-3}–10^{-4} mol L^{-1}. Consequently, compounds with long lifetimes, such as naphthalene and pyrene, are particularly sensitive to the presence of molecular oxygen. Furthermore, oxygen quenching is less efficient in highly viscous media. Oxygen can be removed by bubbling molecular nitrogen (N_2) or argon through the solution, but the most efficient method is the freeze–pump–thaw technique. However, removal of oxygen from biological cells (such as mammalian cells) and tissues is not feasible because oxygen is needed for their physiological functioning.

The excellent sensitivity of fluorescence makes it possible to observe the time-resolved fluorescence of a highly fluorescent emitter that may represent only an impurity of a few parts per million in nonluminescent material. Moreover, nonluminescent impurities can quench the fluorescence of interest, or they can form complexes

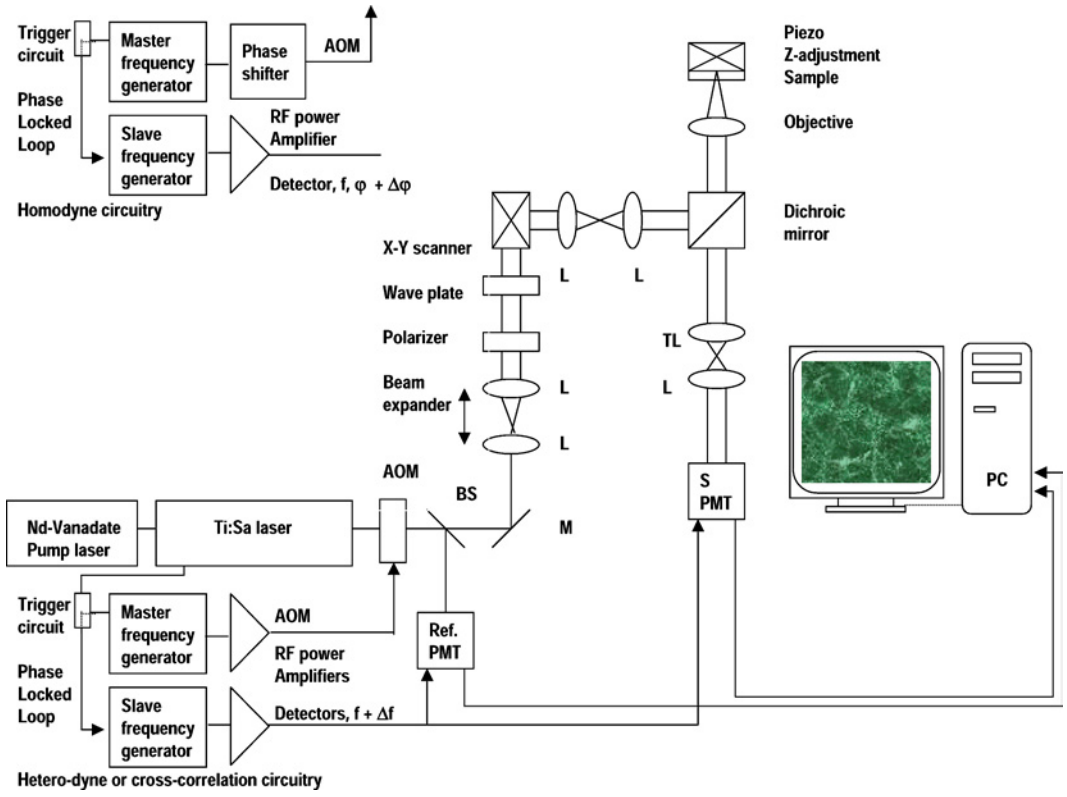

Fig. 4. Schematic of a FLIM homodyne and heterodyne frequency-domain time-resolved imaging set-up. Pump laser may also be a large frame Ar ion laser. BS: beam splitter, L: lenses, TL: tube lens, M: mirror, PC: personal computer with large storage capability and installed digital acquisition electronics, ref PMT and S PMT reference and sample photomultiplier detectors with scanning laser spot. Imaging detectors like MCP-CCD cameras may also be installed. Intensity control via an acousto-optic modulator (AOM) but also Pockels cells or similar may be used. A phase locked loop signal is derived from the laser and triggers the data acquisition. Figure based on set-ups available at the Laboratory for Fluorescence Dynamics of the University of Illinois at Urbana–Champaign.

with the compound under investigation. These processes distort the excited-state kinetics of the studied compound. Impurity distortions are extremely difficult to treat mathematically. The surest—but most time-consuming—way to eliminate this error source is to purify the sample thoroughly.

Solvents

Neat Solvents

For fluorescence spectroscopy, ultra-pure water (H_2O) can easily be produced without any fluorescent impurities via, e.g., a Milli-Q® water system (Millipore; for preparation of ultra-pure water: http://www.millipore.com). Starting with de-ionized or distilled water, several filter and ion exchange cartridges are used to remove dissolved organic material, inorganic ions, and colloidal and bacterial contamination. High quality water, delivered by a properly maintained Milli-Q® system, meets all the requirements of fluorescence spectroscopy. For optimal water quality, a Milli-Q® system should be maintained periodically and if bacterial contamination is observed, the correct decontamination procedure should be applied as prescribed by Millipore. Although freshly produced ultra-pure water has a pH of 7.0, this pH value drops as soon as water is exposed to the lab atmosphere from which it takes up carbon dioxide (CO_2). Because of this pH drift reliable fluorometric measurements on nonbuffered solutions at pH 7.0 are extremely difficult to perform. If allowed, properly buffered solutions can be used. Even with the highest care ions leaching from the container do contaminate the samples over time (see hereafter under *Solvent Containers*).

Many common organic solvents [acetic acid (CH_3CO_2H), acetone (CH_3COCH_3), acetonitrile (CH_3CN), dichloromethane (CH_2Cl_2), cyclohexane (C_6H_{12}), chloroform ($CHCl_3$), 1,4-dioxane ($C_4H_8O_2$),

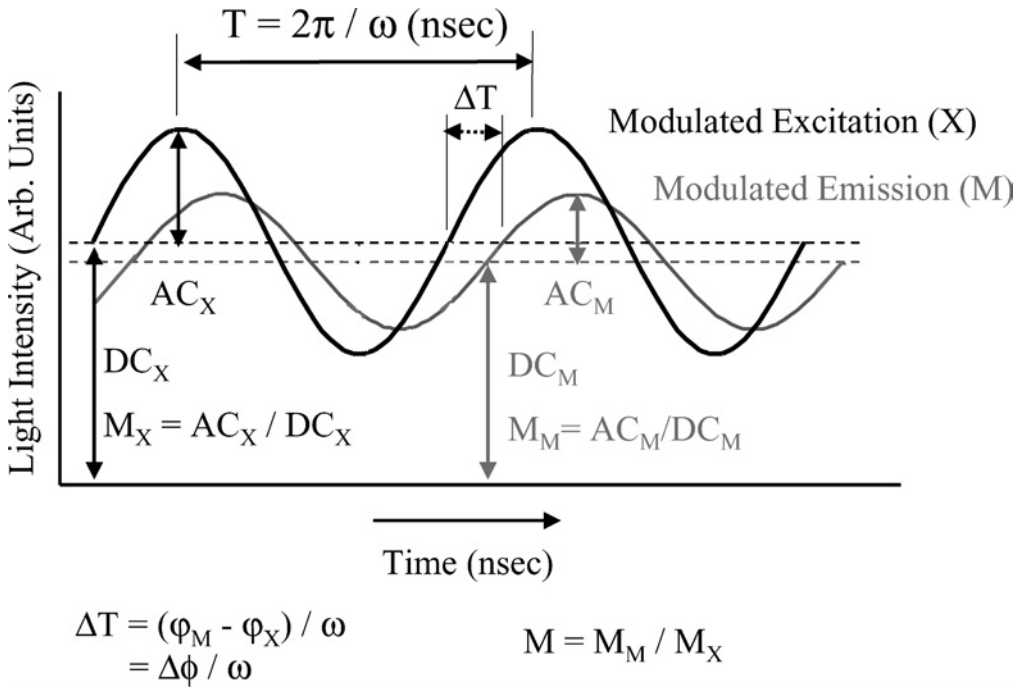

Fig. 5. Principle of a frequency-domain heterodyne or cross-correlation fluorescence lifetime determination. Intensity modulated excitation with a period, T, and angular frequency, ω, illuminates a fluorophore. Decay of the excited state creates fluorescence emission with the same frequency but with a time delay ΔT and decreased intensity. The phase shift, $\Delta\phi$, and demodulation, M, are expressed in the phase differences existing between emission, ϕ_M, and excitation, ϕ_X and the ratios of the varying alternating current, AC, and direct current, DC, signals.

ethyl acetate ($CH_3CO_2C_2H_5$), methanol (CH_3OH), 1-propanol ($CH_3CH_2CH_2OH$), 2-propanol ($(CH_3)_2CHOH$), tetrahydrofuran (THF, C_4H_8O), toluene ($C_6H_5CH_3$), . . .] are commercially available in spectrophotometric or spectrofluorometric grade.

Ethanol (CH_3CH_2OH) arrives in a bewilderingly large variety of different qualities (e.g., the 2003/2004 Fluka catalogue has more than 40 different listings under *Ethanol*). High purity ethanol comes in two main categories: ∼96% (v/v) and 'absolute' or 'anhydrous' [generally > (99% (v/v)]. Ethanol is often *denatured* with additives (2-butanone, toluene, cyclohexane, methanol, 2-propanol, diethyl phthalate, 4-methyl-2-pentanone. . .). Ethanol derived from fermentation might contain some traces of other alcohols (methanol, iso-amyl alcohol) and carbonyl compounds. Ethanol (prepared industrially or via fermentation) sometimes has fluorescent impurities. Therefore, to test the quality of ethanol (or any other solvent), perform the fluorescence test as described in the next paragraph.

The purity of any solvent can be tested in the excitation beam with as high illumination levels as possible. It is good practice before starting any time-resolved experiment to observe the fluorescence signal under standard instrument operating conditions and record the fluorescence spectrum of the blank (neat) solvent with a spectrofluorometer. Occasionally the contamination level is so high that it can be seen directly by the naked eye as a fluorescent beam volume in the cuvette. It must also be noted that the moment a new solvent bottle is opened, the solvent will take up water from the lab atmosphere unless strict precautions are taken to prevent this.

Buffer Solutions

Several buffer ingredients can be purchased as fluorescence free reagents (HEPES, K_2HPO_4, MES, MOPS, potassium and sodium acetate—acetic acid, Tris . . .). Background fluorescence might arise from buffer solutions due to impurities from buffers that are not labeled as "for luminescence" (or similar). If in doubt, check the quality as described for solvents.

Viscous Solvents

To make dissolving fluorophores in viscous solvents [such as ethylene glycol (1,2-ethane diol) and glycerol (1,2,3-propane triol)] easier, the solvents should be gently

warmed as to make them more fluid. This also allows air bubbles to be removed relatively quickly.

Solvent Containers

Even the most carefully prepared solvent or buffer has to be stored sometimes for extended periods in a container. Typically a glass jar or plastic bottle will be used and the solutions are stored in the dark in a refrigerator. The closing cap should be as chemically inert as possible (e.g., with a Teflon lining, not with Para-film). Purity problems may arise from plastic bottle plasticizers and glass bottle leachates as described in reference [21].

For microscopy applications one can construct fluorescence sample holders from cover slips and spacers with low or nonfluorescent glue that does not readily dissolve. It would be easier if standard cuvettes could be placed on the stage but usually the available space is too limited. Care should be taken that during the experiments the sample and reference solutions are placed in ultra-low background glass or quartz cuvettes. A similar remark can be made about plate reader well plates. The plastic surrounding the well may give a fluorescence background which will hinder accurate polarization measurements. Commercially available black plastic plates with low emission and reflection should be used.

Scattering Materials Used as Reference

Glycogen powder should be stored in a well-sealed bottle in a dry place. When stored as a powder in a refrigerator one should let the container warm up sufficiently. Otherwise moisture will condense when the container is opened spoiling its contents over time. Freshly prepared glycogen in ultra-pure water (see *Neat Solvents*) should be kept in a refrigerator. When used immediately small undissolved globules may disintegrate and increase the signal and slowly saturate the reference detector signal of a MPF. Certainly the glycogen solution should not be kept for an extended period on a laboratory bench where bacterial growth will cause autofluorescence.

Ludox (colloidal silica) is more convenient than glycogen: solutions are stable for long periods of time and they do not have to be kept in a refrigerator; moreover, they can be easily diluted or concentrated for intensity adjustments.

Coffee creamer can be used when freshly made from powder. When left standing, it spoils. Milk (diluted) should be avoided, because it sticks to the cuvette walls, decomposes rapidly in a warm environment and consequently makes cleaning of the cuvettes very hard.

Glass bead suspensions create after centrifugation a fairly monomodal dispersion of small beads which tend to stay in solution due to Brownian motion for days.

Protein Solutions

Cuvettes

Cuvette walls consisting of glass or quartz contain charged groups which facilitate protein adsorption to the walls thereby lowering bulk concentrations and altering conformational shape, spectral and polarization properties of attached proteins. Application of Tween 20 (a polyoxyethylene-sorbitan monolaurate amphipathic surfactant) strongly reduces this effect.

pH and Temperature

Denaturation of proteins can be avoided by keeping them as much as possible in their natural environment. For example, for proteins of warm-blooded animals this means a pH between 7 and 7.5 (occasionally up to pH 8) and a temperature below about 40 °C. The higher the temperature, the more a protein will be denatured. During purification of proteins, it is generally better for their stability that they are being kept on ice. Warming up proteins to dissolve them should be avoided, unless the protein is known to be a heat shock factor and hence can tolerate high temperatures.

Buffers

Zwitter-ionic buffers that cannot interact with biological material (e.g., HEPES with pK_a 7.55 at 20°C) are the best choice. HEPES has a low absorption between 240 and 700 nm (important for fluorescence measurements) and is chemically stable.

Shaking

Protein solutions should never be shaken vigorously to dissolve protein particles. Many proteins are fragile and start foaming when shaken. The soap-like foam contains denatured protein which may or may not go into solution and this produces incorrect lifetime and anisotropy values.

Filtration

Filtration of protein solutions is generally not a problem and is often used to concentrate proteins. The

solubility of the protein is a critical factor and other components in the solution may be affected by the filtration. It is also possible that the protein attaches to the filter membrane, resulting in a decrease in total protein amount.

Reducing Environment

The cell environment is reducing. Hence it is recommended to add a reducing agent (0.5–1 mM dithiothreitol or 5–20 mM β-mercaptoethanol) to the solution to avoid oxidation of cysteines and the formation of aspecific disulfide bridges.

Storage

To store proteins over extended periods, it is recommended to add 10–30% glycerol as a cryoprotectant to mimic the low water activity present in the cell. Ten percent glycerol can be added to solutions used for fluorescence measurements, especially when measuring on enzymes that rapidly become inactive in an environment with a too high water activity through formation of inappropriate interactions.

Solubility

Some proteins are indeed rather insoluble. It must be noted that proteins are the least soluble when the pH is equal to the pI. Choosing a pH different from the isoelectric point can increase dramatically the solubility.

Cofactors

It is also important to know if an enzyme needs a cofactor for its proper functioning. This cofactor should be present to guarantee the optimal activity of the enzyme.

Freeze–Thaw

Although "freeze-thaw" cycles are the best method for removing dissolved gases from solutions, this technique should not be used with protein solutions. Freezing and thawing has a severe denaturing effect on proteins.

Physiological Salt Concentration

Finally, often 100–150 mM NaCl is added to protein solutions. Proteins in cells are functional at this salt concentration.

Fluorophore Concentration and Inner Filter Effects

Cuvettes

Radiative transfer is a two-step process: a photon emitted by a donor molecule D is absorbed by an acceptor molecule that is chemically different (A) or identical (D).

$$D^* \rightarrow D + h\nu \tag{3}$$

$$A + h\nu \rightarrow A^*(\text{heterotransfer}) \quad \text{or}$$

$$D + h\nu \rightarrow D^*(\text{homotransfer}) \tag{4}$$

Radiative transfer is observed when the average distance between D and A (or D) is larger than the wavelength. Such a transfer does not require any interaction between the partners, but it depends on the concentration and on the overlap of the donor fluorescence spectrum and the acceptor absorption spectrum. For heterotransfer ($D^* + A \rightarrow D + A^*$), the donor fluorescence decay remains unchanged, but the steady-state fluorescence of the donor decreases in the region of overlap between the donor fluorescence spectrum and the acceptor absorption spectrum. Such a distortion of the fluorescence spectrum is called *inner filter*. However, for radiative transfer between identical molecules ($D^* + D \rightarrow D + D^*$, homotransfer), the fluorescence decays more slowly because of successive re-emissions and re-absorptions. On the other hand, the fluorescence anisotropy decay becomes faster because the excitation energy is transferred to another molecule with a different orientation of the transition dipole moment. Also now the steady-state fluorescence is decreased in the region of spectral overlap. The visually observed penetration depth of the excitation beam into the cuvette solution may be greatly reduced. Inner filter effects are difficult to correct and therefore it is advisable to work as much as possible with dilute solutions (low absorbance). When the use of high concentrations is required, the fluorescence should be monitored in the front-face configuration by using very thin cells. It is recommended that the illuminated surface is oriented at 30° to reduce the amount of stray light reaching the detection system. An example of a top down illumination configuration with polarization compensation is shown in reference [22].

When zero-crossing detection is still used instead of digital acquisition MPF the intensities of sample and reference cuvette should be very well matched (i.e they should not differ by more than 10%). It is recommended to adjust the concentration of the reference cuvette (with the less expensive material and available in larger quantities) to that of the sample. Reference and sample cuvette intensities should be perfectly matched for zero-crossing detectors so they operate on identical gain settings and identical noise characteristics in both reference and sample

channels. Matching to operate with the same gain settings is also recommended for digital acquisition analog-to-digital converting ADC cards.

Microscopy

Because of reduced optical path length much higher fluorophore concentrations can be used when they prove not to aggregate or to be cytotoxic.

Molecules in a Liquid Environment

Effects of Temperature

Molecules in a liquid environment exhibit fluorescence emission properties that may depend on the solvent characteristics. Bulk properties may depend on parameters like solvent viscosity and temperature: the lower the temperature, the higher the viscosity. This in turn has its influence on the molecular rotational behavior: a higher viscosity leads to a lower rotational rate.

Optical (An)isotropy

Polarization effects are studied for e.g. following enzyme binding kinetics, local cellular viscosity, polymer and immobilized molecular orientation. Cuvette-based fluorescence instrumentation comes typically in a 90° (excitation–sample holder–emission) geometrical configuration. With one emission arm left or right in place an L-format optical configuration exists. For two emission arms a T-format geometry saves a factor of two in measurement time.

Fluorescence emission properties of an ensemble of molecules depend on the characteristics of the individual molecules. A single molecule with the absorption moment perpendicular to the excitation polarization direction will not absorb and therefore not emit any fluorescence at all. Maximum absorption takes place when the absorption moment is parallel to the excitation polarization direction. This phenomenon leads to the process of photoselection [2,23].

If a molecule with parallel absorption and emission moments does not rotate between the moment of absorption and the instant of emission (e.g., when embedded in a solid matrix), fluorescence emission mimics excitation. Samples with a random ensemble of molecular orientations possessing identical optical properties in all directions are optically isotropic. When the molecular rotational motion (i.e. the rotational correlation time of a fluorophore) is of the same order as the fluorescence decay time, samples will display optical anisotropy. Faster rotation will average properties: samples will look isotropic. Slower rotation may mean that the fluorescence emission may have decayed completely inhibiting further observations. Bulk samples can display optical anisotropy when their optical properties are not identical in all directions.

Membrane-bound fluorophores in cells will display local anisotropy. Cytosolic fluorophores will show an isotropic behavior. Cells, giant vesicles [24] and suspensions as well as molecules immobilized on surfaces typically display photoselection effects. In microscopy—especially with high numerical aperture objectives—the orientation of the local excitation field has directional properties that deviate from those observed in the typical 90° L- or T-format optical configuration found in fluorometers [25].

Temperature, Condensation, and Polarization Effects

One should be aware that a stock solution taken from a refrigerator has to warm-up to room temperature. Warm-up effects may invalidate any time-resolved measurement until all sample and solvent containers have reached the same temperature. Several important temperature dependent effects can be observed. Temperature influences solvent viscosity and thereby temporal molecular rotational properties: the more viscous the medium, the slower the molecular rotation. In highly viscous solvents like glycerol and ethylene glycol air bubbles are stirred in when mixing. One may add 10% of a less viscous solvent. Addition of a fluorophore dissolved in a small quantity of ethanol or methanol improves homogeneous mixing and reduces formation of stirred-in air bubbles which take a long time to disappear if at all. These air bubbles will give rise to a harder to eliminate scatter signal.

The contribution of well walls has to be checked. If the temperature of each well is checked, one will find in many commercial instruments surprisingly large temperature differences of several degrees centigrade. In addition to the effects discussed above extra effects occur in microscopy on living cells and tissues. These effects relate to autofluorescence, dye leakage, active transport out of the cells and cytotoxic effects [26].

Cuvettes

In cuvettes without liquid mixing, considerable temperature gradients (up to 5°C) can exist within the solution. A Teflon coated magnetic stirring bar will mix the liquid and minimize temperature differences. Special cuvettes are commercially available with a special stirrer bar

geometry that does not obstruct the observation volume. Water vapor condensation on the outside cell wall gives a rather periodic fluctuation in the MPF signal. This stability problem is caused by water droplets rolling down along the cuvette outer wall. To remedy this, one should use a room temperature dry gas or nitrogen flow directed onto the cuvette excitation and emission windows. Another way of eliminating these effects is using a vacuum cuvette.

Microscopy

Typically an objective and stage heater with an overflow of warmed air prevents radial and axial temperature differences between sample and objective surfaces. Temperature differences will change the focus properties.

Photobleaching Effects

Bulk Solid Samples

Prolonged excitation destroys fluorophores. To extend the "life" of fluorophores, one should reduce the illumination intensity as much as possible (neutral density filters can be helpful). When using transparent plastic solid samples one could prop them up or rotate them to expose a fresh volume. After some use they contain bleached channels with a very low signal. Nonetheless, high-quality solid optically transparent single-lifetime standards would be very useful for instrument standardization.

Cuvettes

Photobleaching effects are reduced or eliminated by a metering pump delivering continuously fresh sample to the illuminated volume. Rotating Kiefer cell type cells with a liquid layer spun by centrifugal forces against the inside of the cuvette wall will also alleviate photobleaching.

Microscopy

In microscopy, photobleaching effects can be severe but strongly depend on sample temperature. For example, a fluorescence recovery after photobleaching experiment at 20°C with illumination for 1 hr with 100% (∼1 mW) laser power at the sample of an Alexa dye may not show any bleaching effect. Changing the temperature to 37°C may bleach the dye completely in a few minutes. Consider the following. Suppose 100 μW 514 nm laser light is focused by a 63× oil objective with 1.4 NA. One can expect a fluency density of about 1 kW/cm^2. Remedies against photobleaching like removal of molecular oxygen cannot be applied because the typical animal cell cannot survive without oxygen. Photobleaching of fluorophores in cells has been reviewed by König [26].

Autofluorescence

Another often severe difficulty is caused by the level of self-fluorescence from cellular components [27,28]. Many cell constituents give a substantial autofluorescence background after excitation with 400–500 nm light. The only remedy is to use longer excitation wavelengths so that light absorption by cell constituents is less. This highlights the need for developing probes excitable with visible light—preferably well above 500 nm—for the study of *in vivo* physiological phenomena.

OPTICAL ARTIFACTS

Fluorescence intensity and anisotropy decay measurements mostly use UV, visible and NIR excitation light sources. Hence, the fluorescence emission is also detected in this spectral region stretching from 250 to 900 nm. Intrinsic fluorophores like phenylalanine, tyrosine and tryptophan emit in the UV region. Most dyes are excited and emit more to the red. Currently a limited number of fluorophores emits above 650 nm. Hence, the optical elements have to transmit the same spectral region from UV–NIR. A number of artifacts can occur that one has to avoid or to correct for if unavoidable.

Optical Layouts

The optical layouts of state-of-the-art time-resolved fluorometers for time and frequency domain are shown in Figs. 1 and 2 respectively with typical 90° L- or T-format optical geometries. Analogous implementations for microscopy are given in Figs. 3 and 4. In the following, the observed artifacts caused by the various optical components are reviewed. We follow the optical path progressing from light source via the sample (compartment) to the detector section as shown in Figs. 1 and 2.

Excitation Path

CW Excitation Light Sources

Although modular diode and fiber lasers are making inroads, so far, for frequency-domain fluorometry, an arc lamp constitutes a rather inexpensive light source. It still

gives access to reliable inexpensive excitation, which in combination with an excitation monochromator or a set of interference filters delivers a wide spectral tuning range extending from the UV to the NIR.

For a lamp an optimal current with maximum arc stability exists for frequency-domain measurements. For ageing Cermax lamp arc instabilities increase the data collection time. The rear integrated parabolic reflector creates a high intensity collimated output but burns away with use. This reduces total lamp output over time. Best arc stability has to be determined experimentally and best operating conditions for lifetime measurements can be found in the MPF instrument documentation and are typically in the mid current range. When replacing lamps, be aware that no UV is transmitted by the glass front window present in an ozone-free lamp. This means that no UV excitation for decay time determination of tryptophan or proteins is possible. One should take care installing the proper lamps for the experiment (i.e., UV or non-UV illumination).

Light Emitting Diodes (LEDs) have an ever increasing market share with more wavelengths and higher light outputs becoming available on a regular basis [4,29]. Since the beam extends over a solid angle of 10–50°, a proper excitation lens and diaphragm combination should create a parallel illumination beam to conduct polarization experiments. Overdriving will warm the devices up so that the emission wavelength shifts. Although much cheaper and easier to handle than lasers, the latter have much higher output power in an approximately collinear Gaussian beam. When the financial means and an emission wavelength matching the absorption properties of the sample are available, lasers are clearly the light source of choice.

We refer to several reviews [5,30,31] tabulating the excitation wavelengths, output power, polarization properties and costs. The trend over the past years is to make this equipment not only available to physicists but to a much wider audience in the form of completely automated push-button devices that automatically maintain output, mirror alignment, etc. Nevertheless one should be aware that several properties of these otherwise marvelous light sources can wreak havoc on the lifetime measurements when certain artifacts occur.

Ion gas lasers emit several lines in UV (the more powerful higher current models) or VIS lines simultaneously when no wavelength-tuning prism is installed. It may happen that a multiple UV emitting Ar ion laser operating simultaneously at 351.1 and 363.8 nm but each line with a time varying intensity. Figure 6 shows the MPF response. Only the insertion of a UV 340 interference filter selecting the stronger line eliminates the problem of anomalous multiple decay times for a single-lifetime fluorophore MPF calibration sample.

Laser power output is influenced by mechanical vibrations, beam pointing stability, dust, interaction between transversal and longitudinal laser cavity modes, laser cavity alignment, radiofrequency (RF) pickup, temperature, and polarization effects.

Fluctuations in excitation intensity will cause an increase in measurement time or when mode-hopping occurs phase-locked-loop conditions are compromised and an erratic or zero MPF response may result. A number of CW (Continuous Wave) laser excitation source related phenomena related to impeded MPF operation are listed here to make the reader aware of them. Overviews of remedies for fighting laser cooling water vibration and smaller laser fan induced mirror vibrations, etc. are given in reference [31]. Even the simple fact of a temporary drop in water flow will impede proper cooling and may make quick MPF lifetime measurements impossible due to the increased laser output noise during this period. Water-cooled lasers may even shut down when cooling is insufficient. A buffer volume cooling water with electronic valve should be considered. The alternative is to wait out the low water flow periods.

For time-resolved measurements, the light beam has to enter centered and on the optical axis of the Pockels cell modulator and reference detector beam splitter. As an example consider this real-life situation: a 200-μm narrow laser beam (FWHM) did not enter completely centered and touched the wall of a 1-mm alignment pinhole which was left in place resulting in a slightly off-axis entry into the Pockels cell modulator. This led to various degrees of modulation. Accurately recentering the laser beam with a punctured business card removed the effect. This same configuration also had a related malfunctioning reference detector channel. See below under *Reference Detector Channel*.

Not only mechanical vibrations and optical alignment but also dust specks cause an unstable or even a zero-output CW laser system. The following is a real life situation. A single very minute dust speck in the wrong spot on a laser output window created a very unstable light source from one day to the next. A large frame water-cooled CW Sabre Ar ion laser (Coherent) lost its power to pump a Ti–Sapphire laser in a completely erratic way. On very close inspection (laser goggles!) one could see a minute bright spot on the Brewster window. Cleaning the window according to the manual with lintel free swipes and a small amount of solvent dislodged the dust speck before it could burn in into the optical coating of the output window. After cleaning full power was restored instantly.

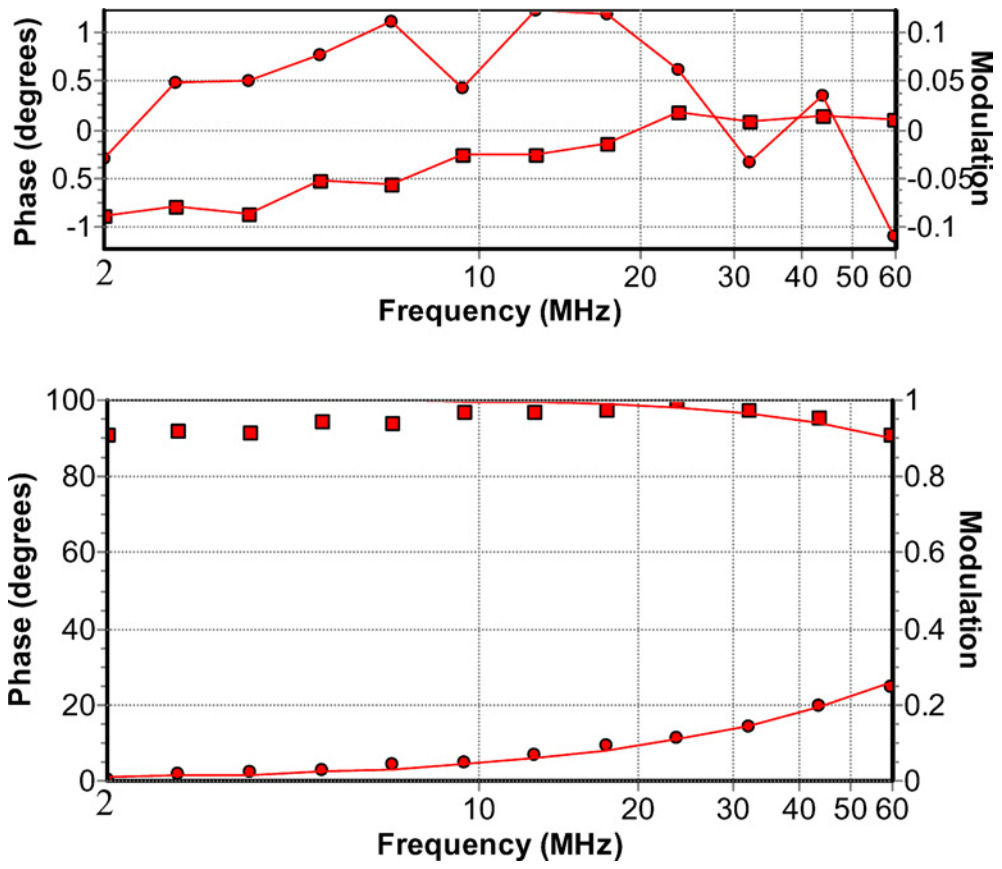

Fig. 6. Example of MPF data collected with multiple UV Ar ion laser line excitation. During data collection laser excitation wavelength switching, intensity and mode instabilities occur. Phase and modulation values indicated respectively by (•) and (■). Upper panel displays residuals.

Sometimes UV-line emitting CW Helium–Cadmium (He–Cd) lasers are notoriously ill-behaving, which causes inoperable MPF setups. In several instances it has been observed that a He–Cd laser operated at 352 nm but alternatingly in two transverse modes TEM00 and TEM01* due to an aging tube. Very erratic MPF data were collected leading to an almost infinite data collection time resulting from excessive averaging. Retuning and intensity optimization helped somewhat. In the end the tube had to be replaced. Probably due to the specific laser head design using a passive air-cooling flow some of these designs are intrinsically sensitive to room temperature variations. As another example a He–Cd laser placed in a sparingly heated room got subjected to seasonal room temperature fluctuations. Each year in spring and fall the optics had to be realigned to keep the MPF system running in a workable but certainly not optimum condition.

Unsuspectingly even laser excitation delivery by single-mode fiber-optic should be scrutinized. The quality of the fiber optic may induce large power fluctuations of up to 30%. When replaced it may be down to 3% improving the signal-to-noise ratio dramatically. Having described several examples of CW laser excitation source instabilities leading to compromised MPF data collection, we now turn our attention to pulsed light sources.

Pulsed Excitation Light Sources

In phase fluorometry a high repetition rate pulsed light source will allow MPF measurements, because the Fourier transform of the excitation contains all necessary harmonics of the base frequency. In principle they do not require an intensity modulator but they may be inserted for obtaining a lower optical pulse repetition rate.

Flash lamps as well as nitrogen and deuterium lamps for SPT with coaxial designs have been reviewed thoroughly [19] and will not be discussed further. They are notorious for their radio frequency (RF) generation. In SPT lamps have mostly been replaced by LED and laser light sources. LEDs are cheap and reliable light sources

but when driven at high current they warm up. Therefore, the emission wavelength may shift. With age their output power drops. This will result in a change in excitation intensity with time [4].

Due to the complex nature of synchroton light sources, up-time is not always optimal. As few synchrotons are around, access may be limited to a few times a year in order to work for a limited period round the clock to collect data. Decreased pulse intensity and injection mishaps can occur. On the positive side it offers a light source with an extremely wide tuning range [3]. Special care has to be taken to water cool optical parts like coupling mirrors. For synchrotron-based MPF it is mandatory that the master synchrotron frequency generator should be set to a nice integer frequency. This allows one to use a low base harmonic frequency of, e.g., a few MHz, which better covers the fluorophore frequency response as compared with just a few higher frequency harmonics. Fractional frequencies create an inoperable phase-locked loop and result in an MFP set-up displaying zero signal levels. Decreased pulse intensity and reduced bunch lifetimes result from a wrong injection. No MPF signal may be observed because the base frequency may be all wrong.

Having been replaced largely by Titanium-Sapphire lasers, dye lasers caused a lot of RF pickup in MPF systems. The RF generated by the cavity dumper drivers from dye lasers requires extensive signal cable insulation, double shielded BNC cables, case grounding, removing ground loops and physically placing the device as far away as the laser table allows from the detection system.

The workhorse light source in many laboratories is the Titanium-Sapphire laser. To bring the typically 80 MHz optical pulse train repetition rate down, a small beam splitter picks off a minute fraction of the output and redirects it to a trigger diode. Small drifts in beam position on the diode create an unstable pulse picker. The best remedy is to reduce the distance between the optical components so beam drift is less of a problem. Pulse picker RF warm-up effects may create side pulses leading to different harmonic content of the excitation. Warm-up or cool-down effects cause a slow drift in laser cavity length and consequently in optical pulse repetition rate. When large enough the phase locked loop reference will go outside its control range and the MPF will not be able to function properly any longer. In small rooms one could open the doors or add extra fans but even so Ti–Sapphire systems may have to be retuned every 15 min. under these conditions. A slow buildup of condensation on the Ti–Sapphire rod due to a malfunctioning temperature control bath on the Ti–Sapphire rod will fairly rapidly lead to a very unstable laser and possibly destroy the rod when proper action is not taken at once. It has been observed that at times during SPT experiments a sudden drop of up to 80% in average laser power may occur with accompanying large changes in pulse shape and disastrous effects on the quality of the collected fluorescence decays (see Fig. 7). Long term drift in laser cavity length is to be suspected. Retuning resets the laser to previous intensity levels and pulse shape.

Excitation Beam Delivery

Direct coupling by a beam steering device is possible for all lasers but the beam should be enclosed for eye-safe and dust-free operation. Using one of the commercial or home-built beam steering devices one should be aware of

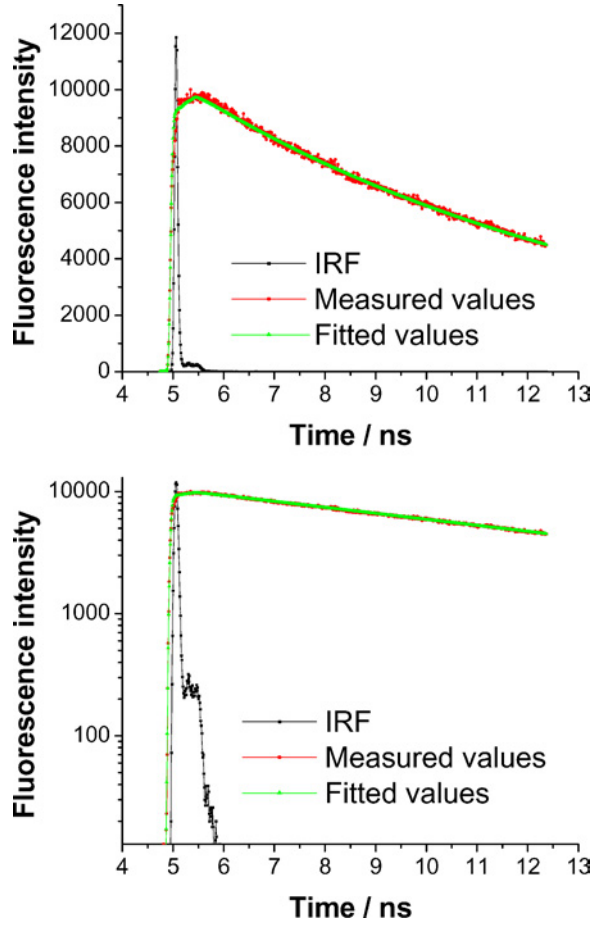

Fig. 7. A dramatic drop in laser intensity (up to 80%) and concomitant pulse shape changes during the collection of the fluorescence decay of 9,10-diphenylanthracene in methanol ($\lambda_{ex} = 360$ nm, $\lambda_{em} = 420$ nm) via the SPT technique lead to artifacts. Shown are the IRF, the experimental and the fitted values (over 740 channels, 10.3 ps/channel) as a single exponential decay ($\chi_r^2 = 2.383$). The weighted residuals and the autocorrelation function are a clear indication of a bad fit.

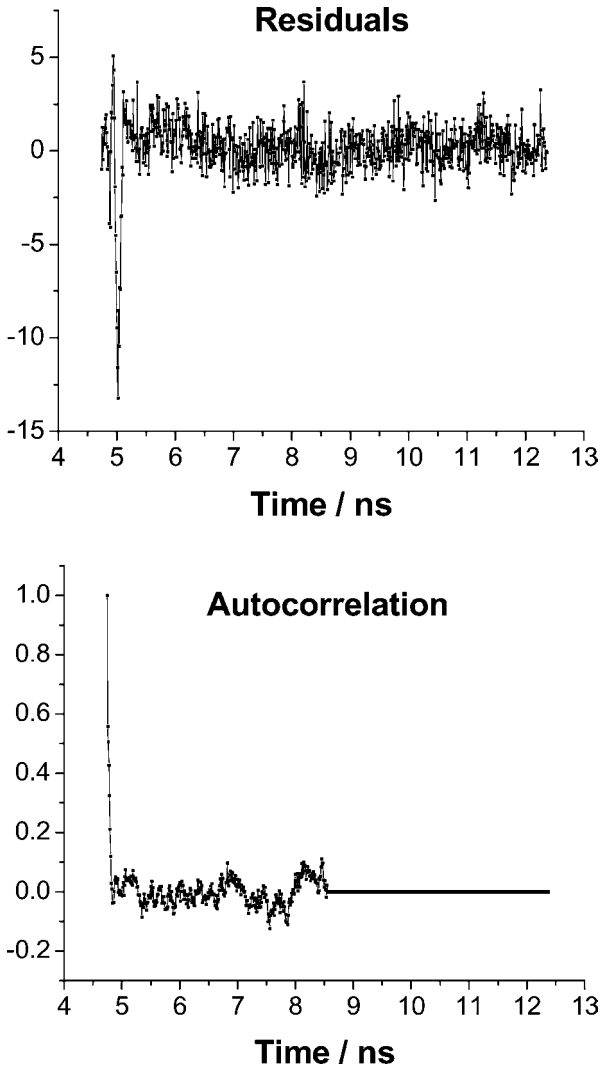

Fig. 7. Continued.

the fact that dependent on the optical orientation of the two mirrors a polarization rotation of the excitation light occurs. A horizontally polarized beam enters the Pockels cell modulator, which results in no light at all coming out of the assembly. It may mean one has to add a halfwave plate, skip the beam steering device or one has to put a laser on its side impeding cooling and possibly against warranty conditions. It has been observed that large dust particles in the beam create intensity fluctuations impeding fast MPF data collection.

Fiber optic coupling is these days the standard for most small frame lasers. They come with a small length of fiber optic (30 cm to 1 m typically) length. They are aligned with respect to the maximum emission of each diode in a fully automatic manufacturing process. When the fiber breaks or is ripped off, a very low unstable illumination results causing very lengthy data collection times if it works at all. If the optical fiber is broken, one can as well buy a new pigtailed laser diode because replacement costs amount to a new device. Transmission of femtoseconds Ti–Sapphire laser pulses through an optical fiber leads to pulse broadening and is reviewed in reference [32]. Direct coupling via mirrors with an all-dielectric NIR low pulse-broadening ultra-fast antireflecting coating is the better choice. Perfectly polarized light is delivered to the microscope sample when a single mode polarization preserving fiber is used with a small frame Ar ion laser.

Optical fibers are made from very high grade materials. Nevertheless one should be aware that several effects may hinder MPF data acquisition. Solarization effects occur when high intensity laser light is focused on the fiber entrance. Over time this may lead to color center formation near the fiber tip. Increased absorption, heat generation and finally destruction of optical coating and bulk material may result. This leads to unstable illumination intensity and an unworkable MPF. Although most fiber materials are very pure, small inclusions may cause scatter and autofluorescence. The fiber optic core and cladding not only contain OH^- ions leading to absorption in the NIR and IR but also small imperfections and trace amounts of impurities. Especially plastic fibers may give a very high fluorescence background and should not be used unless with proper filters. Optical quality glass and quartz constitute the best choice but should be well protected against room light intrusion (black cladding) and a metal coil preventing easy fracture. Coiling the fiber to small diameter will certainly lead to laser intensity loss and sooner or later to fiber fracture, create a minimal MPF illumination of very bad spot quality. This will necessitate replacement.

Intensity Modulation

Several devices are used for changing the intensity of laser excitation light. Acousto-Optic and Electro-Optic Modulators (AOM, EOM), Acousto-Optic Tuning Filters (AOTF) and Pockels cell modulators are devices most commonly found. A brief review can be found in reference [19].

When driven hard with a large signal these devices get heated up so much that it is impossible to touch them. Moreover, over extended periods the high temperatures may reduce the coupling efficiency of the transducer by a loosening of crystal-transducer contact. The efficiency of these devices depends on the frequency used and on the angular orientation of the crystals with respect to the

incoming excitation light. Certain frequencies work very well, others hardly at all reflecting most of the drive signal. A proper 50 Ohm terminator design is a must.

AOM modulators pass several diffraction orders, i.e., reduced intensity light spots, which follow a slightly different path. Therefore they can be eliminated by placing a pinhole at a distance of about 0.3–1 m. These rather large distances which are necessary for proper spatial spot selection produce an increased sensitivity to thermal drift. Bacterial growth over time may cause cooling hose clogging. Addition of a spoonful sodium azide cures this problem.

High-quality Pockels cell devices may have two crystals in series for reducing the half-wave voltage and for compensating thermal drift. For a review of their properties, see reference [33]. They create an intensity variation by altering the plane of polarization that passes through a polarization analyzer. Misalignment of a powerful UV multi-Watt laser beam that heats the transducer sides of the crystals will create very hot internal areas causing repetitive heating–cooling cycles with periods of several minutes. Therefore, careful alignment of the brightest laser spot nicely centered along the optical axis will definitely remedy this effect. A malfunctioning or with no bias voltage applied makes the Pockels cell modulator work at the second harmonic in a strongly nonlinear way, thereby creating a number of even higher harmonic modulation frequencies. Another source of MPF instability can be thermal drift due to crystal heating related to reduced high frequency RF efficiency. Setting up an experiment with a reversed frequency order from high to low reduces this effect. Wavelength dependent angular variations in the beam directions will occur when chromatic effects are not taken into account in the design. Assuming cables are properly connected and all components are functioning, a switched-off bias voltage will give a very small nonlinear response near the bottom of the response curve. Switching the bias voltage on brings the Pockels cell modulator in its more linear response range [33]. With a properly adjusted bias voltage level much improved performance is immediately obtained. A correct optical alignment with a minimum number of bright optical reflections from Pockels cell crystals and windows is mandatory. This can be checked by tracking the spots along the optical path with a punctured business card and by observing the on–off/bright–dim blinking of the center Brewster cross on the card. Perfect optical alignment with a well contrasting Brewster cross is a must to check and optimize performance. Near the center of the crystals the modulating field is strongest. Therefore, one can rather easily reach close to 100% modulation for frequencies where the modulator response is optimum with a narrow laser beam while a lamp source does not reach this high value anywhere in the frequency range. In general for UV operation quartz crystals are used. Unfortunately their efficiency amounts only to about 10% and not to the 60–80% of TeO_2 based devices. Compensating with more laser power may do. Occasionally the electrodes to the crystals loose firm contact due to changes in the bonding material related to a long period of very excessive heating. Also mechanical shock may result in a similar effect. Modulation will be very poor for all frequencies. When all else has been checked it may be worth contacting the manufacturer for a test at the factory.

Beam Splitter

In the excitation path the fused quartz beam splitter directs excitation light to the reference detector. This beam splitter plate has to be very well aligned and firmly in place. Otherwise reference detector signals may deteriorate over time.

Excitation Wavelength Selection

One of the most commonly found artifacts is related to the wavelength selecting device characteristics and orientation. See also *Emission Path* below.

Optical filters operate on the principle of bulk absorption or interference effects. When interference filters are inserted tilted, they show a small wavelength shift in the position of the peak transmission. The shiny side should always face the light source to prevent destruction.

Bulk absorption based optical filters may emit some of the absorbed radiation as fluorescence. This autofluorescence does not so easily influence the reference detector channel but will scatter from the sample and cuvette walls. Tests can be carried out in a darkened room with bright excitation and observe blue, yellow, or pink emission from the side of the filter. Another optical filter with similar properties but from another manufacturer may exhibit far less autofluorescence. The purity of the glass and inclusions apparently play a big role. Proper storage and clean handling are a must.

A synchrotron excitation source creates so much heat that optical components require a water cooled frame. Extended exposure of gratings to bright UV light causes solarization of the coating warranting an inspection and potential replacement at least once a year. Afterwards an order of magnitude more light may suddenly be available again. A dust-free Nitrogen flow will reduce this burn-in effect sharply. Accidentally working with a higher monochromator order changes the wavelength

transmission properties and intensity. It is useful to occasionally check the transmitted color with a business card against the dial reading. Fixing a jammed monochromator has to be followed by a recalibration of the dial with, e.g., a He–Ne laser. Its reading of 632.8 nm should match the dial with narrow slits inserted or selected. Sometimes deviations in MPF lifetime values are caused by a monochromator dial not matching the actual excitation wavelength. Polarization properties and transmission effects do change the transmitted intensity. Sometimes a monochromator cannot be used at all at given wavelengths due to grating anomalies present [34]. In case no information can be obtained from the manufacturer one should test the monochromator with a standard well-known sample.

Acousto-Optic Tuning Filters (AOTF) in Laser Scanning Microscopy

Scatter caused by cellular layers in close proximity to a slide surface or semiconductor support may create a false fluorescence background when the wavelength discrimination by the Acousto-Optic Tuning Filters is not perfect; i.e., stray laser excitation light is in overlap with the fluorescence probe emission excited by a lower wavelength line. Especially MPF time-resolved anisotropy measurements with this type of stray light are nearly impossible.

Polarization Effects Due to Monochromator Magic Angle Configurations

The transmission efficiency of a monochromator depends on the polarization of light, mainly due to the polarization dependence of the monochromator grating. Consequently, the observed fluorescence intensity is dependent on the polarization of the emitted fluorescence, i.e., the relative contributions of the vertically and horizontally polarized components. This problem can be circumvented in the following way. If no polarizer is placed between the sample and the emission monochromator, the light intensity viewed by the monochromator is not proportional to the total fluorescence intensity. To get a response proportional to the total fluorescence intensity, independent of the fluorescence polarization, polarizers must be used under "magic angle" conditions: a polarizer is inserted in the laser excitation path just before the sample and set in the vertical position, and another between the sample and the emission monochromator and set at the magic angle (54.74°). Alternatively, the excitation polarizer can be set at the magic angle and the emission polarizer in the vertical position. To summarize, it is always recommended to use properly oriented polarizers when a monochromator is used to select the wavelength of the emitted fluorescence. For reviews, see references [2,9]. Not taking these precautions for lifetime measurements couples in rotational effects and gives an incorrect lifetime in MPF and SPT measurements. The magic angle conditions are listed here for a number of polarizer orientations: (1) Excitation vertical and emission polarizer at 54.7°; (2) Excitation at 54.7° with the emission polarizer vertical; (3) With the excitation at 35.3° no emission polarizer is required. See under *Emission Path* hereafter why this latter configuration can only be used when an optical filter is used as wavelength selective device. It should not be used with a grating monochromator used in emission.

Short optical pulses of different color follow different paths in a monochromator. This effect is readily observed in SPT and can be eliminated [35].

Polarizer Position

When laser excitation lines with more than about 100 mW are used, the excitation Glan–Thompson (Canada balsam or with a similar material assembled unit) has to be exchanged with an air-spaced Glan–Taylor one. Higher power laser lines should have this latter polarizer with specially antireflection coated exit windows to create no heat stress on these delicate components. When uncoated, thermal stress will cause beam deviations making lifetime measurements impossible. Cracked polarizers may create two or more closely spaced excitation beams which leads to anomalous results especially when the spots alternate in intensity due to heating effects in the crystal.

Raman Background Signals

A persistent signal in fluorescence spectroscopy is the inelastically scattered Raman signal of the solvent, usually water. For a review, see e.g. reference [36]. Inelastic scatter from mostly the O–H stretching vibrations creates a photon with decreased (Stokes) or increased energy (Anti-Stokes). Since both the laser excitation wavelength and the OH vibration have certain fixed values under given experimental conditions, the Stokes Raman signal appears in the fluorescence emission spectrum as a weak symmetric band at a predictable spectral position. A hallmark feature of Raman scatter of water is the occurrence of a symmetric rather broad scatter line with a half width of $\sim 50\,\mathrm{cm}^{-1}$. The symmetric and asymmetric O–H stretch vibrations of water show a band near $3400–3600\,\mathrm{cm}^{-1}$. Subtraction of this number from the excitation wavelength expressed in wave numbers gives the location of the water Raman peak position. An example of

how to calculate the Raman position: (1) express the laser excitation wavelength—e.g., 488 nm–into wave numbers: 20492 cm^{-1}. (2) Subtract the Raman OH vibration located at 3400–3600 cm^{-1} to the red: 16892 cm^{-1}. (3) Reconvert the result to nm: 592 nm. Other solvents like benzene (C_6H_6), cyclohexane (C_6H_{12}), tetrachloromethane (CCl_4) also show strong but much narrower Raman scatter lines. This solvent scatter signal is therefore present in the emission channel unless it is removed with a proper interference filter or emission monochromator.

Lenses

Sometimes a high-quality fused quartz lens selected for very low fluorescence background is accidentally replaced with a lower quality more fluorescent glass lens. UV lifetime determinations become then impossible.

Reference Detector Channel

A particular problem may arise from the fact that the reference detector receives usually more than enough lamp or laser excitation light intensity from the excitation beam splitter. Typically a dual differential measurement is made in MPF. First the sample response is determined against the reference detector, i.e., the excitation source phase and modulation. This is followed by a measurement of the response of the reference cuvette contents again against the reference detector signal. A pathological situation may occur especially with inexperienced users who tend to reduce the reference detector cathode voltage to the absolute minimum to prevent detector and ADC signal saturation. This causes a loss in proper response at once accompanied with anomalous MPF readings since the reference detector now operates outside its linear response range. A minimum cathode voltage level of several hundred volts is recommended. Nonetheless a strong reduction in signal level is necessary to prevent reference PMT saturation. This can be achieved by inserting a neutral density filter when available or a stack of also wavelength neutral and independent copper screens in front of the detector. When UV illumination is used the neutral density filters must be quartz. Copper screens work rather well when the laser beam has a diameter of several millimeters. When the laser beam diameter is very tiny (a few hundred microns) it may hit and be obstructed by a single-copper strand. In this latter case the addition of a scattering piece of plastic scatters and widens the beam. In combination with a total of 2–5 copper screens to reduce the amount of excitation light seen by the reference detector this filter assembly provides a sufficient signal level for a proper reference detector signal.

Occasionally when a frequency-domain fluorometer is also used as a steady-state fluorometer, the triangular Rhodamine 6G or similar quantum counter like a Rhodamine 101 cuvette [2] may still be in place. The light passing through this cuvette towards the reference detector is inadequate to serve as a reference signal. First it has a certain fluorescence lifetime and since the concentration is very high it is certainly not a single lifetime. When this quantum counter cuvette sits repositioned in such away as to reflect the excitation light directly to the reference detector it receives a mix of very strong reflected excitation light with a small fluorescence signal. This is not an ideal situation.

Infrequently it has been observed that a very narrow laser beam of 200 μm (FWHM) was about completely blocked by a single strand of a neutral density copper screen filter. The spurious light passing was then optimized for collecting data but the reference detector cathode area was apparently only receiving some stray photons leading to anomalous electron transit paths inside the detector giving strong phase and modulation artifacts. Insertion of several folded layers of transparent plastic acting as a diffuser eliminated the effect.

Sample Compartment Area

Turret

With adjustable turret stop positions one has to be sure they are not ill-adjusted. A misaligned stop position leads to obliquely incident light. This creates a difference in the detector cathode area illuminated and consequently differences in electron paths and observed phase and demodulation values for MPF. In SPT this may show up as a time-shift between the instrument response function and the sample decay. Additionally an increase in scattered excitation light contributions to the total signal may be observed and concomitantly an increase in emission background from bulk absorption wavelength selecting filters.

Magnetic Stirrers

Vigorous stirring naturally equilibrates the sample temperature but fragile proteins may denature as foam on top of the solvent. Visual inspection of the absence of an air bubble vortex further reduces the scattered excitation intensity.

Cuvettes

Herasil and Suprasil type deep-UV quartz cuvettes are without any measurable intrinsic background signal.

However slightly less expensive Pyrex glass cuvettes when used, e.g., to measure UV excited components show a quite detectable background fluorescence which although not readily observed by eye causes havoc with single-lifetime tests.

Reflected laser light may at times create a large background and reflections as was observed for hemoglobin lifetime determination with a MPF MCP-PMT set-up [22]. Only a black quartz walled cuvette gave a proper reduction in stray light.

Small rectangular (2×10 mm or 3×10 mm) cuvettes save sample volume. When the focused excitation grazes or hits the inside walls, very strong scattering occurs. This leads to spurious detector signals or an increased probability of background emission from filters. Adsorbed material may partially denature giving rise to different lifetimes. Furthermore, this type of mishap may create hot spots on the illuminated detector area causing early local cathode fatigue or destruction.

For FLIM performance tests the same type of standard cuvettes and fluorophores can be used when the optical configuration allows this. For point-like lifetime measurements on a microscope stage, one should take care that the illuminating beam enters the cuvette exactly normal to the bottom surface. Failing to do so creates strongly deviating recorded phase and demodulation values. The presence of 45° dichroics changes the direction of polarization of the light passing but should maintain the principle plane. Laser excitation light is usually perfectly linearly polarized when delivered with a polarization preserving single mode fiber at the sample stage. Insertion of a quarter wave plate between e.g. the AOTF and the fiber entrance creates circularly polarized excitation. Upon emission detection again a selection occurs for a given polarization direction to pass to the detector.

Sample and Reference Cuvette Concentration

Highly concentrated samples still can be used for lifetime determination when a top illumination geometry—which also takes care of the proper polarization orientation—is used [22].

Dilution of a stock solution of a reference compound (or scatter) is to be preferred over the direct addition of a couple of crystals of a standard fluorophore (like *p*-terphenyl or POPOP) or a minute amount of scatterer (like glycogen powder). Typically the initial measurements are incorrect but within a couple of minutes when the measurement is repeated the results get worse and worse (see Fig. 8). The reason is that the glycogen solution globules or reference fluorophore crystals slowly dissolve over time. The final result is a reduced penetration of the excitation light, which creates a cathode illumination spot that moves away from the spot illuminated by the sample upon repeated measurements. Left overnight and once again reducing the concentration to the proper level will often deliver correct lifetime values.

Alternative Sample Holders: High Pressure Cell and Plate Reader

Manufacturers of high pressure cells—typically designed to go to a maximum of about 13 Kbar—can supply a selection of small round quartz (or square-base 7×7 mm) bottles with a content of about 1 cm^3 that can be sealed with a polyethylene cap by slipping it over their round neck. Only the highest quality material with few if any inclusions, discontinuities and certainly without discoloration can be used. An applied high pressure may crack the container and spill its fluorescence contents in the pressure transducing liquid. When left to dry, background signals from the deposited wall material will go into solution the next time and surely derail lifetime measurements. The excitation beam should hit a round bottle center-on to reduce reflections. As mentioned when a cap breaks during an increase in pressure the inside of the high pressure cell compartment has to be meticulously cleaned and not left standing to dry out. In the latter case prolonged cleaning with hot solvents in a sonicator bath or with dilute acids is necessary to remove this ever returning fluorescence background from e.g. diphenyl hexatriene which readily dissolves in the ethanol pressure transducer medium. Typical symptoms are an initially correct reading but after proceeding for several hours an initially highly puzzling background shows up which is way higher in intensity than the looked for membrane or protein fluorescence decay signal. This may be going on for weeks on end.

Lifetime and anisotropy measurements with bulging quartz or sapphire windows can only be carried out with proper calibration and internal polarizers.

In plate readers background signals from the plastic walls is a prevalent problem. Black plastic gives a reduced background. To increase sensitivity further longer lifetime compounds can be introduced into the wells to discriminate against these spurious signals.

Emission Filter Orientation

Emission absorption type filters inserted next to the sample or reference cuvette have to be placed normal to the emission optical axis. These filters have typically a thickness of between 1 and 3 or even 5 mm. The more tilted and thicker they are, the worse the differential

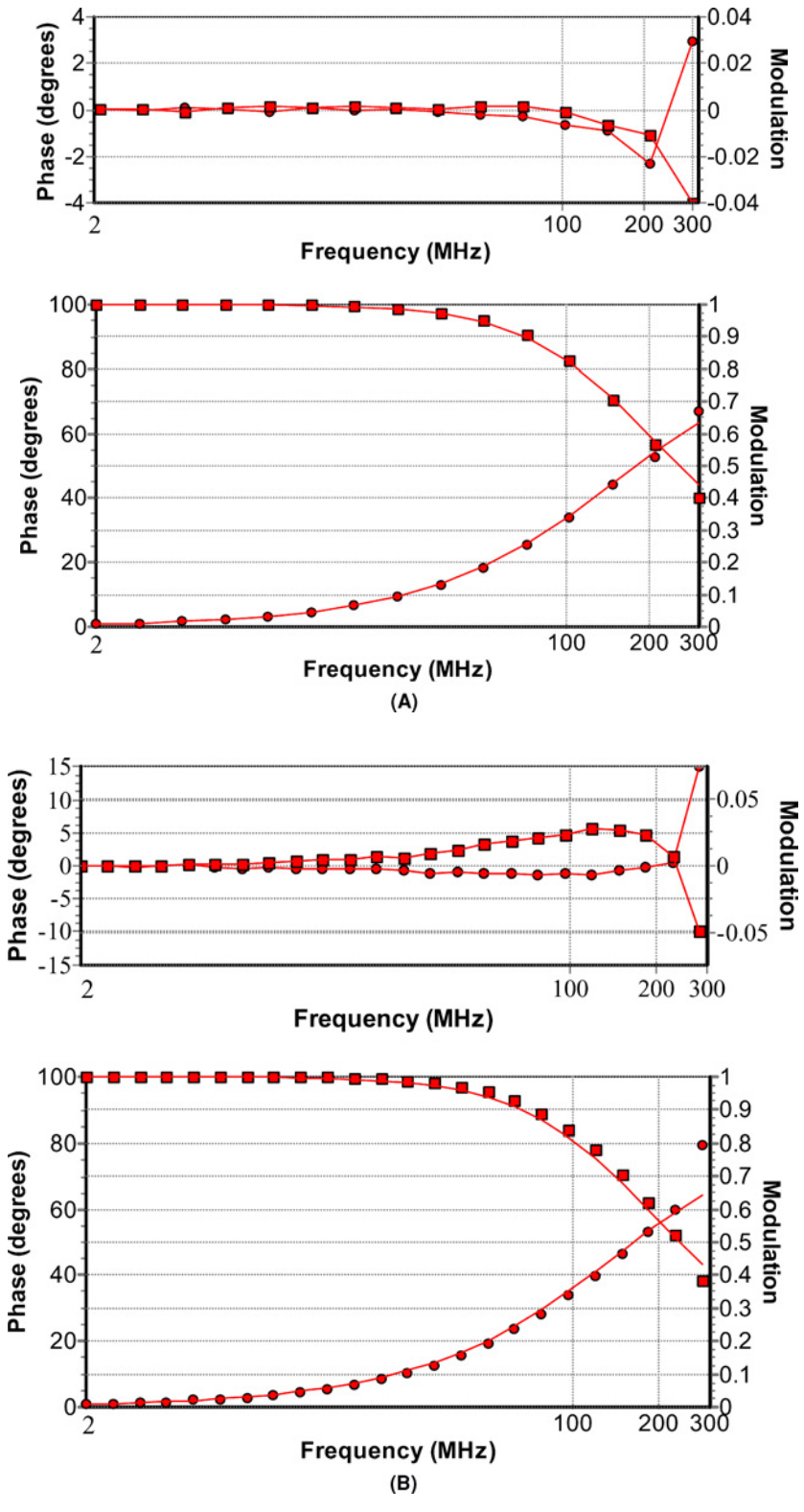

Fig. 8. Example of too-quickly-prepared reference cuvette solution. (B) taken approx. 10 min after (A). No stirrer activated. The very small particulate fluorophore crystals keep dissolving. Phase and modulation values indicated respectively by (•) and (■). The residuals are indicated in the Smaller panels.

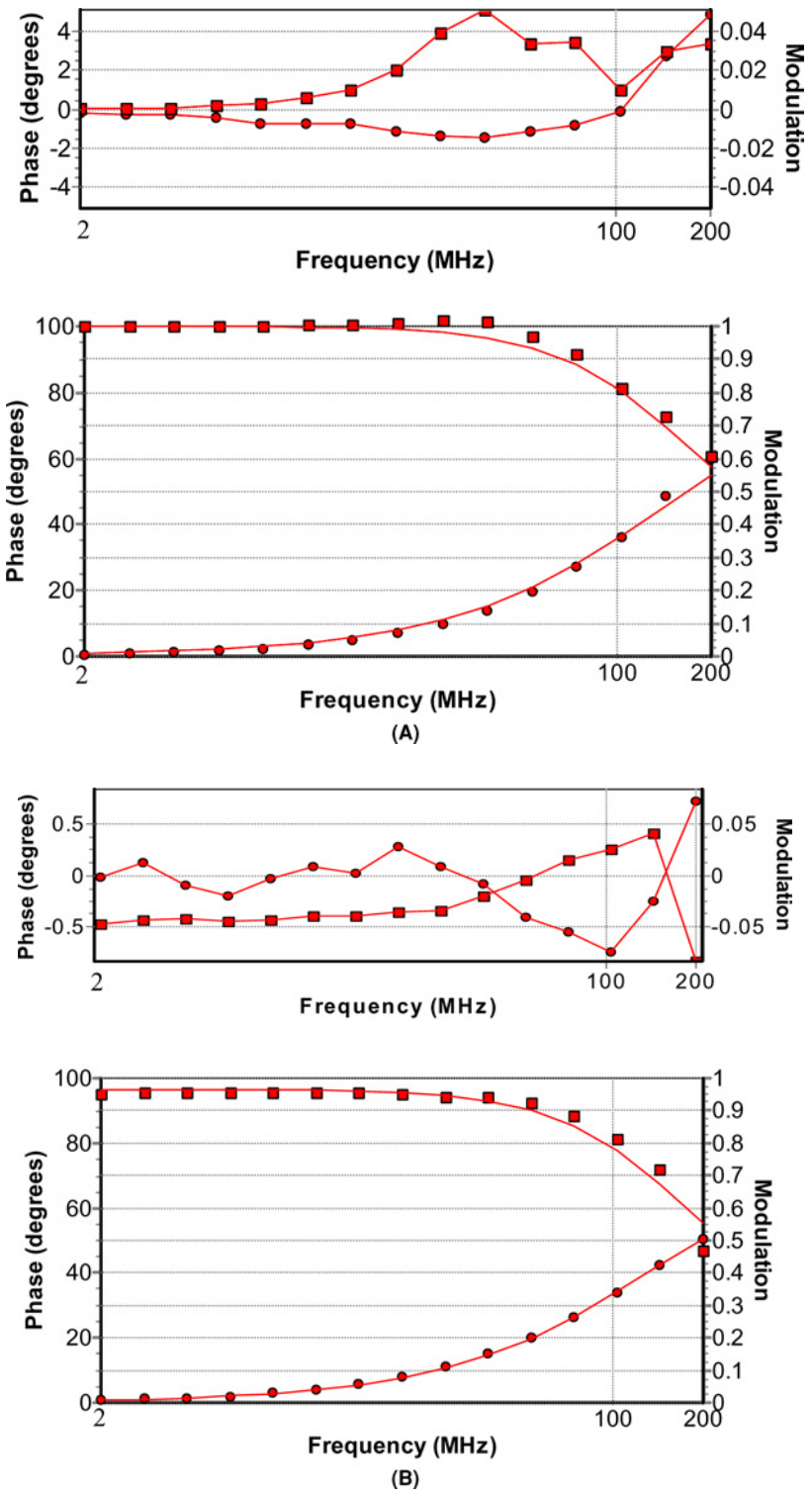

Fig. 9. (A) shows a 2-mm thick absorption type optical filter tilted towards the emission detector. (B) shows the same filter tilted towards the turret. The thicker and the more tilted the optical filters the more distorted the curves are. The effect is caused by the sample and reference cuvette emission or scatter reaching different detector cathode areas. Phase and modulation values are indicated respectively by (●) and (■). The residuals are indicated in the Smaller panels.

beam displacement on the emission detector cathode. This strongly influences the observed lifetimes (see Fig. 9).

Emission Path

Scattered Excitation Light

It can become nearly impossible to resolve fast decay components when scattered light is strongly present in time-resolved fluorometry. The dilemma at the moment of data analysis will be: is it really scattered light or are there one or several very short fluorescence decay times? For time-resolved anisotropy measurements all scatter contributions have to be rigorously removed.

Checking for the absence of scattered light for anisotropy data collection could be done as follows in MPF. In a scatter–scatter solution configuration increase the amount of scatter compound only to the water or buffer solution containing sample cuvette. Measure against a dilute scatter solution in the reference cuvette. Excite at an elevated intensity. With the emission filter under test inserted next to the sample cuvette observe the MPF detector response. When no changes are seen in phase or modulation values, the emission filter is serving its purpose. An example of a small amount of scattered light passing through an emission filter or a very short lifetime component is shown in Fig. 10. In this case the addition of an extra fixed value 1 ps component is recommended.

Scattered light contamination may be a serious problem, specifically when weak fluorescence from strongly scattering samples is being monitored. It is not always easy to totally remove (by a double emission monochromator and appropriate filters) the light scattered by turbid solutions or solid samples. The use of an extra scatter function can then be used in the curve-fitting analysis of SPT data. Figures 11 and 12 show the effect of scatter contamination during an SPT experiment. An unacceptable fit was obtained when a mono-exponentially decaying function was used to fit the time-resolved fluorescence of erythrosin in methanol (Fig. 11). When scattered light was taken into account via an additional scatter term in the decay law, a much improved fit was obtained (Fig. 12).

Polarizer Orientation: Magic Angle Settings and Polarization Scramblers

The fluorescence emission, which may be polarized, reaches the grating of an installed emission monochromator. The grating passes vertically and horizontally polarized light differently. This influences the measured fluorescence decay times and distorts all polarization measurements. By using magic angle conditions in excitation and emission this polarization bias can be circumvented [2,9]. Another way to remove this polarization bias may be placing a scrambler consisting of small angle quartz optical wedges in front of the emission monochromator. Unfortunately these scramblers only work well when the illuminated wedge area is large. When desperate, setting the complete monochromator in a magic angle orientation on a laboratory stage may do.

Light Collection: Lenses and Mirrors

UV absorbing and fluorescence emitting lenses made of glass or crystalline quartz should not be present. They generate a fluorescence background signal. Large solid angle emission collection mirrors may result in incorrect polarization values. The same is true for short focal length lenses. In microscopes with moderate and high Numerical Aperture objectives similar polarization value distortions occur and have to be corrected for.

Emission Spectral Range Selection

Calculate in advance where the water Raman is expected and select a filter that blocks it. Tilted filters act like a plane-parallel plate and shift the beam on the detector cathode surface. They should be placed straight up. Often only a filter is placed in front of the sample cuvette to select the proper fluorescence signal. To perfectly match the optical geometry one may place a blank in front of the reference cuvette. For GHz experiments with a MCP-PMT this is a must. Femtosecond pulses passing through e.g. a 1 mm thick quartz plate show a time delay due to optical path length and refractive index effects [37–40]. This can be used beneficially to calibrate the frequency response of the set-up. For anisotropy measurements filters have to be tested rigorously for blocking excitation stray light, because polarization measurements are easily made invalid by leaking stray light.

Optical Shutters

Light leakage from incoming room or sun light can be a problem as well in time-resolved fluorometry. A loosened flange when hit by direct room or sun light may pass a very small amount of stray light directly into the detector. A quick check is provided by darkening the room. Use a flashlight to find the light leaks. Burs have to be removed. Black silicone and black electricians tape can be used to seal off the leak.

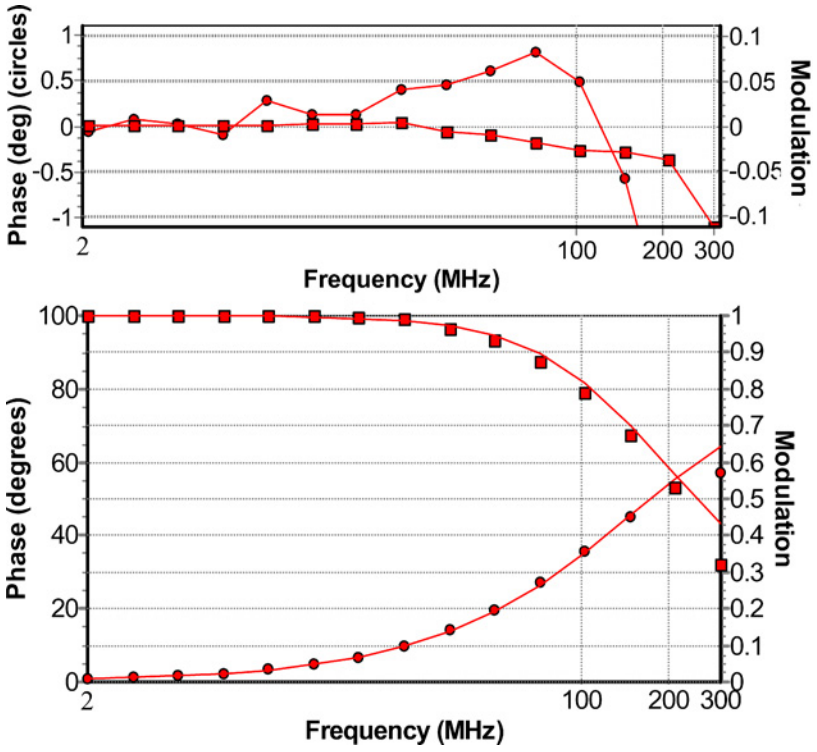

Fig. 10. Judicious choice of emission filters inserted vertically creates a frequency response with a slight very short lifetime or scatter component passing through the emission filter. Both phase and modulation points dip somewhat at the highest frequencies. Inserting a better absorption or interference type emission filter from another manufacturer may further improve the data but can also deteriorate the result. Phase and modulation values are indicated respectively by (●) and (■). The residuals are indicated in the Smaller panels.

Detector Quartz Envelope

The round shaped vacuum enclosure and photons bouncing from the grill cause stray signals. As for steady-state fluorometers photomultiplier detectors to be used for time-resolved fluorometry have to be tested for spurious effects. The optically transparent vacuum envelope does fluoresce when hit by high energy electrons. A thin wire grid is placed between the cathode and the envelope. It is kept at ground potential. Earlier designs by Hamamatsu had a zig-zag thin round wire and post design. Later this design was replaced with a thin flat about 1 mm wide metal strip design. As a result on average more detectors show an increase in anomalous electron paths caused by incoming photons scattered from the thin strip sides and have to be rejected for MPF applications.

ELECTRONIC ARTIFACTS

Misalignment, wrongly calibrated or malfunctioning electronic equipment may cause a series of sometimes hard to track difficulties, which can only be traced by meticulous eye for detail in the excitation path, the sample area, the emission path and electronic processing. An increase in noise means increased measurement time with concomitant sample bleaching and reduced spatial and temporal detail. Following the usual optical path from excitation to detection, we list here a series of commonly encountered difficulties and their remedies.

Light Sources

Short- and long-term instabilities of the SPT instrumentation can cause the excitation pulse profile to vary between the measurement of the instrument response function $E(t)$ [or the reference decay $d_r(t)$ in the reference convolution method (see below)] and the sample decay $d_s(t)$. This will invariantly result in unacceptable fits. The alternate recording of d_s and E (or d_r) averages both d_s and E (or d_r) over the entire collection period. In this way the excitation profile drifts are compensated for.

Pulse picker and cavity dumper electronics generate optical pulse trains with a repetition rate reduced from about 80 MHz to typically 2 or 4 MHz or even lower. This allows a better coverage of the complete time (or frequency) response of a nsec fluorophore. Previously RF interference effects for SPT were discussed in reference [19]. Similarly for MPF these effects are reviewed in reference [41].

For laser cavities common sources of noise and drift are caused by temperature changes in the experiment room. In actively cooled large frame laser systems lowered water flow results in near boiling cooling water and cooling water turbulence. In small frame air-cooled systems insufficiently insulated cooling fan vibrations lead also to laser cavity mirror instabilities, which are usually not properly compensated for by even completely automated systems. With Ti–Sapphire systems the automatic control may run out of its range leading to the false belief that the system is still operating properly. Secondly, the reference diode triggering the phase-locked loop for the frequency synthesizers may drift outside the control band of the synthesizer, e.g. a drift larger than 100 Hz above and below the set "magic" frequency which ties laser light source frequency and detection electronics triggering together. Origins may be positional and orientational drift of the beam spot on an externally placed reference diode. Often this can be solved by placing the diode closer to the beam exit. This type of drift may also cause a diode RF amplifier to saturate when one has set it too close to its maximum amplification level when beam wandering causes a slow or sudden change in diode signal level. A neat way to check system performance is the addition of

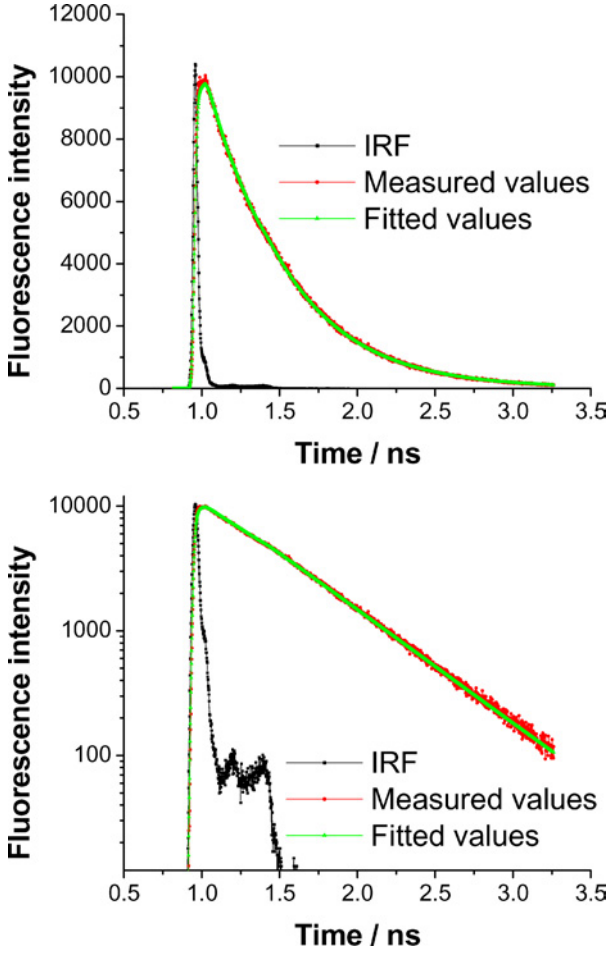

Fig. 11. Scattered light contamination in SPT experiments. Fluorescence decay analysis of erythrosin in methanol ($\lambda_{ex} = 543$ nm, $\lambda_{em} = 540$ nm). Shown are the IRF, the experimental and fitted values (over 1500 channels, 1.6 ps/channel) as a single exponential decay ($\chi_r^2 = 1.990$). The weighted residuals and the autocorrelation function are indicative of an unacceptable fit.

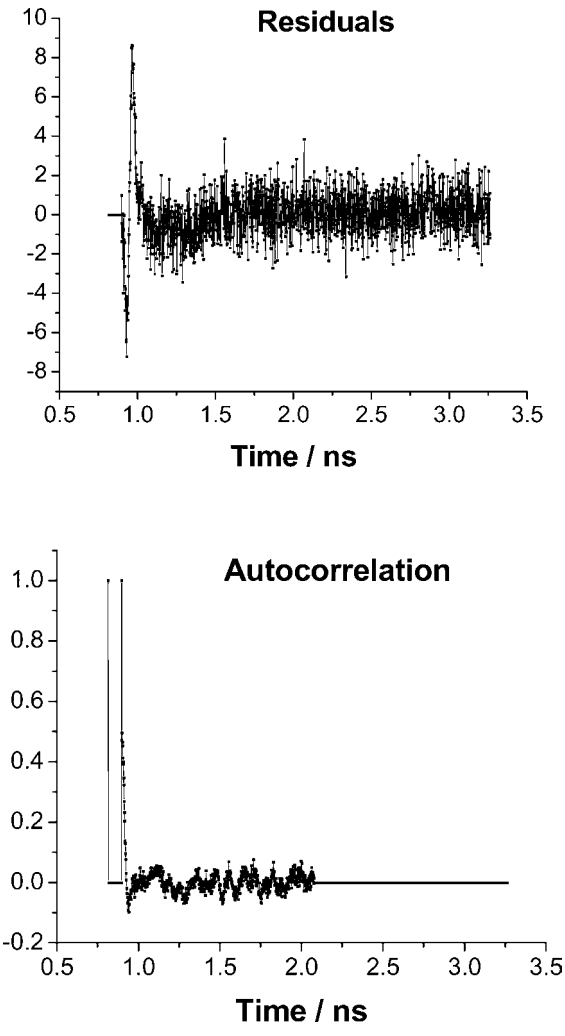

Fig. 11. Continued.

a pulse frequency monitor. Super-heterodyning systems have been described that eliminate in-phase light source noise by shifting it outside the 1 Hz second stage filter width [40].

Intensity stability of diode lasers is excellent compared with water-cooled large frame ion laser [42]. High drive currents may cause heating of these devices and their failure [4]. Also increased mode-hopping will occur leading to output and trigger instabilities.

LEDs are modulated by direct current modulation. For increased illumination intensity high drive currents may be used but this will cause an emission wavelength drift due to thermal effects and result in a shortened lifetime [4].

A well-known phenomenon in ageing compact Cermax ceramic arc lamps is a reduced intensity due to reflector burn-off accompanied by an increase in arc wandering. Intrinsically not nearly as intense as laser light sources they require the use of a monochromator or filter for excitation wavelength selection. Stepper motor jitter may cause a drift in excitation wavelength, which should be cured by proper grounding and avoiding ground-loops. At a certain moment data collection and signal integration times to reduce the signal noise increase so much that a lamp has to be replaced before it is actually dead. On the other hand when the arc moves to a new spot it will be initially rather unstable for several hours. However, good arc stability returns once it settles into its new spot.

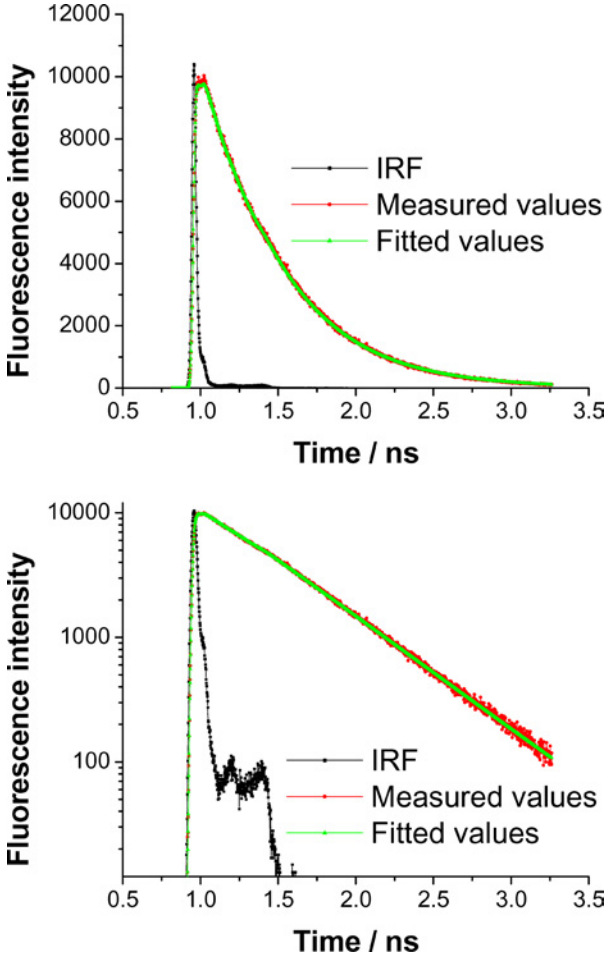

Fig. 12. Same experiment as in Fig. 11, but now a monoexponential plus an extra scatter function is used to fit the time-resolved fluorescence. The resultant fitted values, weighted residuals, autocorrelation function, and $\chi_r^2 = 1.075$ are all indicative of a much better fit.

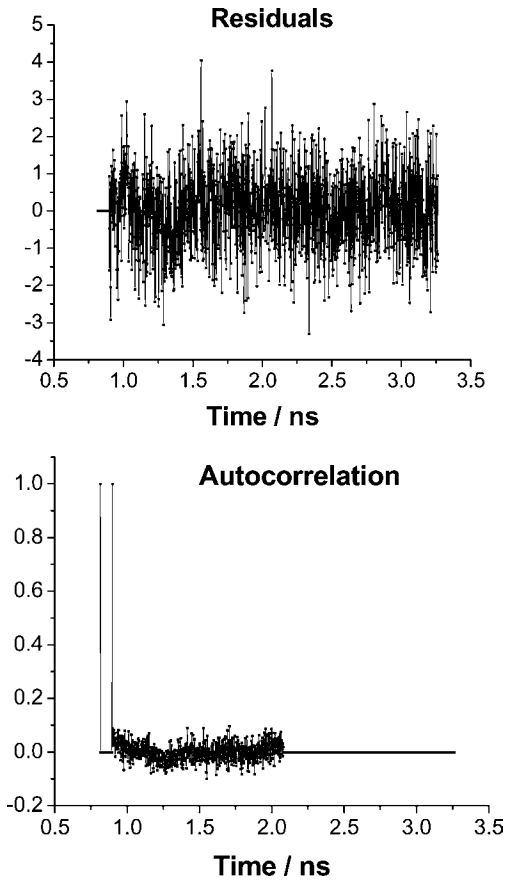

Fig. 12. Continued.

Frequency Generation

The radio-frequency modulation signals generated by a pair of phase-locked synthesizers is amplified and sent to modulator and detectors via BNC (Bayonet Neill-Concelman) coaxial cables. For GHz MPF instrumentation they have to be replaced by higher quality coaxial sma (Sub-Miniature Assembly) connector cables with better microwave RF shielding properties.

Cable configuration is very important. Well known are cases where an effort is made to bundle the signal carrying BNC cables near the instrument together so they look neat and out of the way. This may cause very serious interference and inoperable MPF instrumentation. Very strong RF driving signal carrying cables should not be tied together with weak TTL (transistor-transistor logic) Phase Locked Loop signal and detector signal cables. Therefore the strong driving signals should not be near the signal collection BNC cables and spatially well separated. Cable related issues for SPT have been described in reference [19].

Frequency synthesizers(signal generators have to be selected with the utmost care.

When an MPF instrument malfunctions, phase stability and harmonic noise characteristics from synthesizers may have to be checked. This procedure with an external mixer is described in detail for the measurement of the harmonic pickup and noise properties [41,43]. Since noise is the major source of potential frequency instabilities in frequency-domain instrumentation it has received the most attention. Generally instrument suppliers have thoroughly tested their adequate behavior. As a reminder: disconnecting an RF amplifier while on will result in immediate destruction or malfunctioning of the synthesizer output and should be avoided at all times. Phase Locked Loop electronics is another source of RF pickup and instabilities. A 400–500 MHz or even better several GHz digital oscilloscope allows rapid checking of proper performance of these devices and the phase-locked loop signals.

A major source for malfunctioning phase fluorometers is a laboratory reconfiguration with concomitant RF amplifier mishaps. Generally these devices work as expected. Once BNC signal carrying cables are disconnected even for a fraction of a second from their output connector the RF output section of these amplifiers is immediately destroyed. Occasionally still a much reduced RF output is present but is usually not sufficient. Output signal checks can be made with a 50–100 W 50 Ohm terminating resistor on the input of the oscilloscope. No RF board repair is usually recommended. The best solution is complete replacement of malfunctioning devices.

Excitation Intensity Modulation

All RF modulators—AOM [44], EOM: Acousto-Optic Tuning Filter and Pockels cell for example—have optimum windows for their frequency response with additional "sweet spots" at a limited number of higher frequencies. Especially for these sweet spots the driving signal impedance match is often not optimum leading to an increased heating of the installed crystals. To reduce thermal drift in resonance frequency manufacturers may have added cooling assemblies. With proper tuning of a cooling bath circulator stability of 0.1°C can be obtained. One should be aware that bacteria growing in the cooling tubes—also in the invisible internal cooling coils—will cause over a period of days to weeks a severe increase in thermal drift. Adding a small amount of a bactericide like sodium azide will remedy this.

A source of thermal drift in a Pockels cell is a malfunctioning 10–100 W 50 Ohm impedance matching terminating resistor. This leads at higher frequencies to an impedance mismatch and an increase in reflected RF drive signals. Figure 13 shows a typical MPF curve. The best way to check this is performing tests with first the detector shutters closed measuring the instrument response at each individual selected frequency followed by a scatter-scatter measurement. A correct measurement looks like Fig. 14. With similar materials in sample and reference cuvette position phase and modulation should be very close to zero and one respectively. When operating normally the higher frequencies and existing sweet frequency spots may show a reduced RF driver efficiency and may cause substantial heating of the 50 Ohm terminating resistor. This heat may cause thermal drift causing an initially rapid change in phase and modulation response, which has to be averaged out over many repetition cycles. Best practice in this case may be to start at the most offending highest frequency and let the unit warm up. Then stop and restart the sequence with warmed up electronics running the frequencies from high (several hundred MHz or GHz to low values (a few MHz or kHz).

A Pockels cell modulator's response is quadratic with respect to the applied voltage [33]. When the modulator bias voltage is not present it may be a malfunctioning power supply but also an accidentally switched off bias voltage for alignment purposes or drive signal cables having been switched. Checking the cables and replacing with another power supply typically cures the problem.

Frequency-Domain Detection

Special optical conditions may cause electronic effects inside the detector when electron paths differ between sample and reference cuvettes and their associated optical filters. Systematic anomalies on the emission side are usually severe and rather hard to correct unless standard test procedures supplied by the manufacturer help in tracking the origin.

Several detectors are in use: nonimaging devices like PMTs and MCP-PMTs as well as imaging detectors like array detectors [45], CCD cameras with MCP intensifier

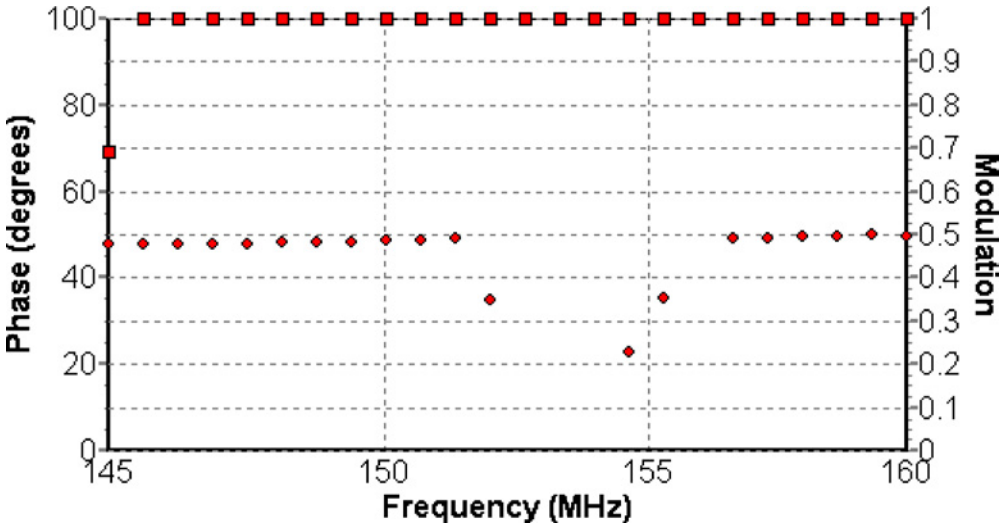

Fig. 13. Example of the influence of a broken 50 Ohm terminating resistor causing impedance mismatch and a partially reflected Pockels cell modulator drive signal. Phase and modulation values are indicated respectively by (●) and (■).

and streak cameras. Each of them has its own set of peculiarities that one has to deal with.

Nonimaging Detectors

MCP-PMT detectors have the fastest picosecond time response and a small color effect. With normal use in 1 year time these devices may become a factor of 100 less sensitive due to intensifier wear-out. Since their replacement costs run into tens of thousands of euro (dollars), most phase instruments are equipped with reference PMT or diode detectors. A very useful feature is commercially offered electronic overload protection packaged together with the detector(s). Exposure to high light intensities even with the high voltage switched off has to be avoided. An external RF AC/DC power splitter and high quality low

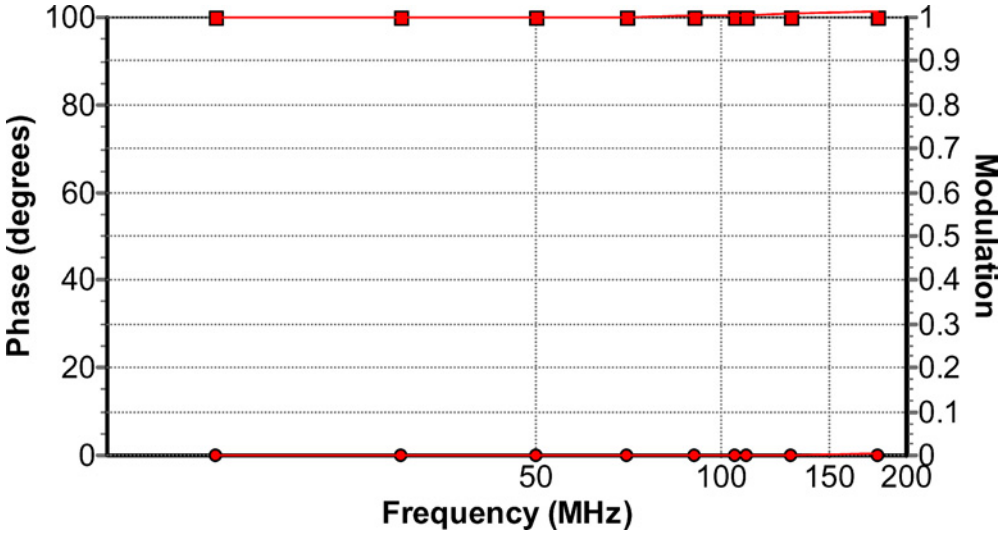

Fig. 14. Example of a test where both in reference and sample cuvette a scatter solution is present. This test is typically carried out after a RF-pickup test with the emission shutter closed and before a test with standard fluorophores. Data collected with a MCP-PMT working up to 10 GHz will show a very short picosecond scatter lifetime. Phase and modulation values are indicated respectively by (●) and (■).

crosstalk double balanced mixer [37,39,40] perform the frequency down conversion in heterodyne detection. This is necessary due to the high internal MOhm resistance.

PMT detector response and MPF data collection is compromised when optical artifacts exist as we have seen above. Also side-on PMTs possess a position dependent sensitivity but have much reduced color effects (see below) as compared with end-on PMTs [19]. By placing and moving a small pinhole over the detector surface one can detect the best spot with highest frequency response. Contrary to end-on detectors one should rather speak about a sweet cathode band located on the cathode tip closest to the first dynode. To reach magic angle conditions in an emission channel sometimes the emission monochromator is propped up on a laboratory stage at the proper angle. Normally the PMT house collection should be kept horizontal for frequency-domain data. When a tilted elongated spot is illuminating the cathode area, severe artifacts may turn up and should be avoided at all cost. Sometimes in instruments where no emission monochromator is installed the detector house is loosened from its support base or the base is removed. It lowers the detector and places it at a slight angle. This practice should also be avoided. For small instrument compartments where PMT detection is added outside the support frame, the detector houses should be kept horizontal and well supported by laboratory stages. A change in cathode orientation produces phase and demodulation variations. When photons reach the cathode surface primary photo-electrons are emitted. Dependent on the cathode spot hit, the electrons follow different paths through the vacuum of the PMT. Electron transit times vary most across the tilted cathode surface and much less along its rectangular surface [46]. For this reason side-on tubes are mounted horizontally on the instrument. As an added benefit the instrument is also more compact. Relocating the illuminated spot towards the tip of the cathode, i.e., translation of the side-on detector housing varies the frequency response and can be used to maximize it. Near the tip of the cathode closest to the first dynode a response of 1.4 GHz has been observed but with strong resonances and rapidly declining at the highest frequencies. This "poor man's" solution to reach a GHz PMT frequency response is certainly not as elegant as a MCP-PMT. PMTs from different manufacturers have been tested. Most have an unacceptable erratic and noisy MPF response with Hamamatsu devices positively performing. A rapid way to destroy the detector base circuitry is accidentally switching RF drive signal and anode signal output BNC cables. Switching modulator and detector RF driving signal carrying cables will usually cook the internal 50 Ohm terminating resistor and nearby electronics. Occasionally a 1 kV blocking capacitor does not work properly anymore and has to be replaced by the manufacturer. Using an oscilloscope one should see a spiky detector dark signal and an increase in amplitude with some modulated light allowed to reach the detector surface. Both internal as well as external gain modulation is feasible.

In order to prevent photoelectrons reaching the quartz PMT envelope, which is at ground potential, a grounded wire grid is placed in between the cathode and the envelope. In the past this grid consisted of a wire and post design. The wires being round and very thin. Later on this construction was replaced by a strip-like design with straight thin edges. On average this thin edged strip design is not as good for phase fluorometry as the earlier wire and post design. More detectors in a batch seem to have to be rejected for a spurious frequency response probably due to a larger contribution from scattered stray photons.

Differential heating of internal 50 Ohm terminating resistors in sample and reference detector housing guarantees a drift in signals. In moist environments or after a mechanical shock electric contacts may have deteriorated. It is good practice to repeat under identical conditions the original calibration tests provided by the manufacturer. Similar results should be obtained. When this is not so the manufacturer should be contacted for further testing at the factory and possibly replacement of defective components.

New users are sometimes distracted by sample preparation or software issues and leave the detector exposed to very high room light or excitation light intensities. They may accidentally forget to close a sample compartment cover, having defeated or bypassed a protective cover interlock or detector shutter when it has been set to manual control thereby blinding and saturating a detector. Another way to reach this very bad situation is exposure to full lamp or laser power from a reflective surface like a still in place triangular quantum counter cuvette. Once this has happened excessive noise is generated by the detector and meaningful measurements become hard to take for the rest of the day. The best remedy is to close the detector-protecting shutter and leave the detector at high voltage on overnight. The next day the system may have recovered and removed the large quantity of electrons created earlier in the bulk of the cathode and dynodes. In extreme cases several days are required to reach acceptable dark signal levels again. Naturally the detector cathode and dynode surfaces age rapidly in this way since the amount of available electrons in the cathode and dynodes is limited. A protective electronic shutter for Avalanche Photodiodes (APDs) [47] may proof useful for above detectors as well and commercial alternatives are available and highly recommended.

Detector base arcing is a potential source of RF noise in MPF. This effect can only be observed in the pitch dark with dark-adapted eyes as a faint blue shine. This arcing is caused by insufficient insulating properties of the detector base. Hamamatsu PMT bases are completely free of this effect even at the highest applied cathode voltages of −1250 V for the 1 1/8 inch (28 mm) diameter side-on PMTs. The take home message is: somewhat cheaper replacements are not always better. Typically from a manufacturer supplied batch only the best detectors are selected for incorporation into a lifetime instrument. PMTs like the Hamamatsu R928 or the R3896 with higher sensitivity are used. Applying 500–700 V cathode voltages to the much smaller 1/2 inch (13 mm) diameter PMTs readily destroys them due to internal arcing. The color effect (see below) is rather small and constant with respect to wavelength.

Detector resistor chain electronics has to be tuned via trim potentiometers to the mid-point of their linear range of their response curve. Failing to do this will result in strong harmonics detection [33]. Another form of RF spurious signal is generated by the power supplies favored for their small size and therefore directly incorporated into the PMT housing. Operating, e.g., around 47 kHz, this power supply switching frequency and its higher harmonics may show up as pickup noise even at several hundred MHz in the raw PMT house output signal. Fast Fourier Transform digital acquisition with its very narrow digital filter usually eliminates this noise contribution. Nonetheless a software selected megaHertz range frequency may show an anomalous response. Closing the detector shutter with no optical signal present may still give a nonzero response. Select in this case another modulation frequency. A spectrum analyzer helps in tracking the exact system component causing the trouble. With age and when malfunctioning the photomultiplier power supply and dynode resistor chain characteristics can be checked with a volt meter, an oscilloscope and spectrum analyzer and replaced when necessary. Still another source of noise is 50 or 60 Hz line interference. It is good to realize that harmonics of the line frequency may be found up to several MHz due to resonance effects. Currently MPF sampling beat frequencies of 400 Hz or even 10 kHz for strong signals may be in use for speeding up measurements and reducing total data collection time. Detector gain modulation and mixing is done by addition of an internal RF circuitry to the resistor chain electronics [33]. Also external RF mixers can be used to obtain down conversion of the high frequency information to a lower frequency. Details are described in reference [43]. The value of this lower frequency has increased over time. Initial instruments used a center frequency well below 100 Hz, e.g., 24, 38, 42, or 63 Hz avoiding at all cost the 50 or 60 Hz line frequency or one of its harmonics passing through the electronic or software filters.

Reference or emission path photodiodes properties—although more robust—may change over time due to ageing. Similar to PMT detectors correct protection against excessive light is useful. High frequency devices have a 0.1 mm^2 sensitive area and misalignment or thermal drift of an impinging narrow laser beam may readily give increased noise in the reference signal or partially burn away the sensor area. Since they are not very expensive compared with PMTs and MCP-PMTs, replacement is usually not an issue. When emission signals are high enough, photodiodes can be used. An RF AC/DC splitter with external so-called double balanced RF mixer with −120 dB or lower port cross-talk in combination with an RF amplifier has to be used. Port cross talk between signal port and intermediate port will result in many additional harmonics related to the drive signal to show up in the down-converted detection frequency. This can be readily checked with a spectrum analyzer usable to several GHz. Dependent on their frequency response, rather longer than shorter emission lifetimes can be retrieved.

Imaging Detectors

A review of imaging detectors has been presented earlier [48]. Instrumentation is now available from several commercial sources and MCP iris effects have been overcome by application of a conducting NESA film [49]. Without such a film the modulating signal reaches the center of the intensifier much later due to a high resistance. Still most applications have been developed for the frequency domain.

Time-Domain Detection

A very good reference is the Becker and Hickl website with time-response and after-pulse information for currently commercially available PMTs, MCP-PMT and APDs [50]. End-on PMT and MCP-PMT detectors are typically used in SPT. As mentioned already the PMT cathode response is not identical over the surface. Sweet spots exist with variations in electron transit time. Noise pulses originating at the various dynodes with lower amplitude can be removed by a properly set lower level discriminator level. A high discriminator level will eliminate pulses created by cosmic ray created particle showers.

Nonimaging Detectors

Avalanche photodiodes (APDs) do typically not provide enough gain by themselves and require additional signal amplification. Their pulse response is also not suited for the shortest femtoseconds and picoseconds duration pulse response but their high quantum yield is unsurpassed.

Photodiode detectors also require additional amplification even more so as compared with an APD. One example for MPF is described in reference [51].

PMTs show several systematic error effects, which can be corrected or should be avoided. The cathode illumination spot should be stable. The instrument response function (IRF) cannot be properly determined with loosely positioned or inclined and slipping units. Changes in the cathode area illuminated create systematic errors. Lacking IRF trustworthiness makes in such a case the calculation of the shortest femtoseconds and picosecond fluorescence lifetimes impossible. Only a fixed (vertical) sample position will give reliable analysis results.

Pulse Pile-Up Effect

In the SPT technique it is important to keep the number of detected fluorescence photons ("stop") small compared to the number of excitation pulses ("start"), [10,11,19]. If the number of "stops" per "start" is small ((5%), the probability of two "stops" being detected per excitation pulse is negligible. The Time-to-Amplitude-Converter (TAC) will only register the arrival time of the first "stop" pulse and the second "stop" pulse will not be detected by the TAC. Consequently, the counting statistics will be distorted. Since only the first (early) "stop" is recorded and all possible consecutive "stop" pulses go unregistered, the resulting fluorescence decay will appear shorter than it actually is. This effect is called the pulse pile-up effect. The simplest way to avoid the pulse pile-up problem is to reduce the mean fluorescence count rate to 1% or less of the excitation frequency.

Linearity of Time Response of the TAC

The linear time response of the TAC is most crucial for obtaining accurate fluorescence decays. The response is more linear when the time during which the TAC is in operation and unable to respond to another signal (dead time) is minimized. For this reason, it is better to collect the data in the reverse configuration; the detected fluorescence photon acts as the "start" pulse and the detected excitation pulse (delayed by an appropriate delay line) as the "stop" pulse.

Insufficient forced air cooling may cause drift in the Constant Fraction Discriminator (CFD) by overheated electronics.

Dependence of the Instrument Response on Wavelength. Color Effect. Reference Convolution Method

The transit time and the transit time spread in standard PMTs depend significantly on the wavelength of the incident photon. This dependence is much reduced in MCP-PMT detectors, which exhibit much faster time responses. Using normal PMTs, this produces a time shift between the sample fluorescence signal observed at the emission wavelength λ_{em} and the signal from the reference scattering solution measured at the excitation wavelength λ_{ex}. In SPT experiments, the reference scattering solution provides the time profile of the exciting pulse (the instrument response function, IRF), and in MPF experiments, the phase shift and modulation of the fluorescent sample are measured with respect to the reference scattering solution. The so-called color effect arises because the fluorescence and reference signals are measured at different wavelengths. In SPT experiments, if the wavelength dependence consists only of a zero-time shift, this can be corrected simply by using a time-shift parameter or a time-shifted IRF in the curve-fitting analysis program of the SPT data. In MPF experiments, if the wavelength dependence only results in a frequency-independent time shift, this time shift can be experimentally determined and its value can be used to correct the phase and modulation data before analysis [52].

However, a more vexing problem [11] is that in addition to the wavelength dependence of the PMT transit-time and transit-time spread (or jitter) (color effect), other timing errors may arise from the dependence of the PMT response upon the position of the illuminated area of the photocathode (targeting), and from the monochromator temporal broadening.

The most efficient way of overcoming this difficulty is to use a reference fluorophore (instead of a scattering solution). The reference compound should have a monoexponential fluorescence decay, and the reference and sample decays should be recorded under identical experimental conditions (λ_{ex}, λ_{em}, optical and electronic settings). Therefore, the reference must be excitable at the same λ_{ex} as the sample and it should emit fluorescence at λ_{em} used for the sample [53].

In an ideal SPT experiment, the time-resolved fluorescence profile of the sample, $d_s(\lambda_{ex}, \lambda_{em}, t)$, obtained by

excitation at wavelength λ_{ex} and observed at wavelength λ_{em} is the convolution of the measured excitation profile (i.e., the IRF) $E(\lambda_{ex}, \lambda_{em}, t)$ and the true sample decay (i.e., the fluorescence δ-response function) $f_s(t)$, i.e.

$$d_s(\lambda_{ex}, \lambda_{em}, t) = E(\lambda_{ex}, \lambda_{em}, t) \otimes f_s(t) \tag{5}$$

where $\otimes$ denotes convolution. An accurate recovery of the fluorescence parameters of $f_s(t)$ requires the instrument response function $E(\lambda_{ex}, \lambda_{em}, t)$. Unfortunately, $E(\lambda_{ex}, \lambda_{em}, t)$ cannot be measured directly. Experimentally one can measure $E(\lambda_{ex}, \lambda_{ex}, t)$ (at the excitation wavelength with a scatterer) or possibly $E(\lambda_{em}, \lambda_{em}, t)$ (by switching to λ_{em} as excitation wavelength) and these functions are used instead of $E(\lambda_{ex}, \lambda_{em}, t)$ in the model parameter estimation procedures. However, these experimentally determined functions differ from $E(\lambda_{ex}, \lambda_{em}, t)$. In the *reference convolution method*, the decay of a reference compound, $d_r(t)$, is recorded at the same instrumental settings (λ_{ex}, λ_{em}, optical and electronic settings) as used for the sample decay, $d_s(t)$. Then the parameters of a modified function $\tilde{f}_s(t)$ are obtained from the experimental fluorescence decays of sample, $d_s(t)$, and reference compound, $d_r(t)$.

$$d_s(t) = d_r(t) \otimes \tilde{f}_s(t) \tag{6}$$

If the fluorescence of the reference emitter decays with a single-lifetime τ_r, then $d_s(t)$ is given by

$$d_s(t) = d_r(t) \otimes \left[f_s(0)\delta(t) + f_s'(t) + \tau_r^{-1} f_s(t) \right] / \alpha_r \tag{7}$$

where $\delta(t)$ is the Dirac delta function, $f_s'(t)$ denotes the time derivative of $f_s(t)$ and α_r is a scaling factor. The weights w_i (see *Artifacts Related to Data Analysis*) used in the SPT data analysis with reference convolution are

$$w_i = \{d_{s,i} + [f_s(0)/f_r(0)]^2 d_{r,i}\}^{-1} \tag{8}$$

where $d_{s,i}$ and $d_{r,i}$ denote the experimental decay data of sample and reference emitter, respectively, and the index i refers to the ith channel in the multichannel analyzer. The weights w_i are adjusted during the curve fitting procedure because they contain adjustable parameters. The reference convolution method is completely general in that a suitable function $\tilde{f}_s(t)$ can be derived for any model described by $f_s(t)$. Since none of the measured decay data are altered in any way, a rigorous statistical assessment of the quality of fit is possible (see *Artifacts Related to Data Analysis*).

A time-shift between the recorded sample, $d_s(t)$, and reference, $d_r(t)$, fluorescence decays is still possible in SPT measurements using a reference fluorophore because the light paths of the two decays may have a slightly different length. Remember that light travels (*in vacuo*) 0.3 mm during 1 ps. A difference in optical path length of a few mm between sample and reference generates a time shift between their respective decays of several ps. For fluorophores with psec lifetimes recorded with a time resolution of less than 1 ps per channel, this can be a significant time-shift (several channels) [54]. These small variations in optical path lengths between $d_s(t)$ and $d_r(t)$ can be due to differences in refractive index, physical sample placement, or cuvette dimensions. The 1-cm path length in standard fluorescence cells may already introduce a time spread of several tens of picoseconds. Fluorescence from a smaller spot can give rise to smaller optical path length differences. These resulting zero-time shifts can be accounted for in the data analysis.

When using MCP-PMT detectors, the color effect is considerably reduced so that a scattering solution can be used as a reference, but for the measurements of very short decay times, the monochromator temporal broadening can still induce timing errors. This effect can be reduced by using a monochromator with a relatively small number of grooves (typically 100 instead of 1200 grooves per mm) [55].

Imaging Detectors

Usually streak cameras [56], position sensitive delay-line detector [57], and MCP intensifier CCD camera combinations are found [58], but also multianode MCPs [59]. The reader is referred to these references for further detail. The main issue is sensitivity. The faster the data collection, the less pronounced the photobleaching effects will be.

ARTIFACTS RELATED TO DATA ANALYSIS

Data Analysis Strategy

In order to distinguish the model for an intricate physical system, time-resolved fluorescence experiments are carried out under different conditions (pH, excitation wavelength λ_{ex}, emission wavelength λ_{em}, coreactant concentration, quencher, temperature, and so on). In single-curve analysis, the fluorescence decay traces are analyzed individually, and a proposed model is tested by the consistency of the recovered parameters (mostly exponential decay times τ and their associated scaling factors α). A subsequent analysis of the parameter estimates provides the parameters of interest, e.g. the rate constants of the excited-state reaction. This conventional approach, though adequate in many cases, fails to take full advantage

of relations that may exist between individual decays. The simultaneous or global analysis of multiple decays uses (and tests) those relationships by keeping some model parameters in common between various related experiments. Examples of global data analysis in the frequency-domain are given in reference [60] and for FLIM in reference [61]. This type of analysis imposes directly the model on the actual decay data. The advantages of the global analysis method are the improved model-discrimination capability and the accuracy of the parameter estimates in comparison to single-curve analysis. For example, in the standard global analysis, the decay times τ can be held in common (i.e., linked) between decays collected at various emission wavelengths. However, in many instances, the τ values will vary between related experiments and hence cannot be linked. This is, e.g., the case where changing the concentration in a system forming intermolecular excimers leads to changes in the decay times τ. The sets of $\{\alpha, \tau\}$ are thus the empirical descriptors of the fluorescence decays. This means that one should fit directly for the more fundamental underlying parameters, which determine τ, that is, the rate constants. By estimating directly the primary parameters of interest in a single-step analysis of the entire fluorescence decay surface, the scope of global analysis is extended. This fitting procedure is known as global compartmental analysis [62]. The fundamental parameters in global compartmental analysis are rate constants, translational and rotational diffusion coefficients, Förster energy-transfer distance between donor and acceptor, activation energy, enthalpy and entropy of activation, spectral parameters related to absorption and emission, etc.

The recommended strategy in fluorescence decay analysis should be as follows: start with single-curve analysis and then progress to standard global analysis (in terms of $\{\alpha\hat{i}, \tau\hat{i}\}$) to finish with global compartmental analysis. The first step (single-curve analysis) should not be skipped, because it allows one to weed out rogue (unacceptable) experimental decay traces and to have an idea of the number exponential terms (compartments) needed. In some cases one can proceed directly from single-curve to global compartmental analysis (when no empirical parameters are linkable).

Least-Squares Approach in the Determination of the Fitting Parameters

In this section, we assume that all possible causes of artifacts due to sample preparation, optics or electronics, as described above, are ruled out.

It should be first recalled that the most widely used method for the analysis of data in both pulse and phase-modulation fluorometries is based on nonlinear least-squares [63]. The basic principle of this method is to minimize a quantity, which expresses the mismatch between data and fitted function. This quantity is the reduced chi-square χ_r^2 defined as the weighted sum of the squares of the deviations of the experimental response $R(t_i)$ from the estimated ones $R_c(t_i)$:

$$\chi_r^2 = \frac{1}{\nu} \sum_{i=1}^{n} \left[\frac{R(t_i) - R_c(t_i)}{\sigma(i)} \right]^2 \tag{9}$$

where N is the total number of data points and $\sigma(i)$ is the standard deviation of the ith data point, i.e. the uncertainty expected from statistical considerations (noise). ν is the number of degrees of freedom ($\nu(N - p$, where p is the number of fitted parameters). If ν is large (as is always the case in SPT measurements), the value of χ_r^2 should be close to 1 for a good fit.

In the *single-photon timing technique*, the statistics obeys in principle the Poisson distribution. The expected deviation $\sigma(i)$ is then given by to $\sqrt{R_c(t_i)}$ but often approximated by $\sqrt{R(t_i)}$ so that the expression for χ_r^2 becomes

$$\chi_r^2 = \frac{1}{\nu} \sum_{i=1}^{n} \frac{[R(t_i) - R_c(t_i)]^2}{R(i)} \tag{10}$$

The quantity χ_r^2 has a precise statistical interpretation beyond that of a number which when minimized gives the "best" fit. The chi-square distribution depends on the number of degrees of freedom ν. Since most statistical tables compile $\chi_{\nu,\alpha}^2$ values only for $\nu \leq 100$ and since for SPT data ν is always larger than 100, it is convenient to compute the standard normal deviate Z_{χ^2} corresponding to χ_r^2:

$$Z_{\chi^2} = \sqrt{\nu/2}\left(\chi_r^2 - 1\right) \tag{11}$$

Since Z_{χ^2} is standard normally distributed, the theoretical probability that Z_{χ^2} exceeds a certain value can be obtained from tables of the standard normal distribution.

In practice, initial guesses of the fitting parameters (e.g. preexponential factors α and decay times τ in the case of a multiexponential decay) are used to calculate the decay curve; the latter is reconvoluted with the instrument response for comparison with the experimental curve. Then, a minimization algorithm (e.g. Marquardt's method [64]) is used to search the parameters giving the best fit. At each step of the iteration procedure, the calculated decay is reconvoluted with the instrument response function $E(t)$ (or the decay $d_r(t)$ of a reference compound).

In *phase-modulation fluorometry*, no deconvolution is required: curve fitting is indeed performed in the frequency domain, i.e., directly using the variations of the phase shift Φ and the modulation ratio M as functions

of the modulation frequency. Phase data and modulation data can be analyzed separately or simultaneously (i.e. globally). In the latter case the reduced chi-square is given by

$$\chi_r^2 = \frac{1}{\nu}\left\{\sum_{i=1}^{N}\left[\frac{\Phi(t_i)-\Phi_c(t_i)}{\sigma_\Phi(i)}\right]^2 + \sum_{i=1}^{N}\left[\frac{M(t_i)-M_c(t_i)}{\sigma_M(i)}\right]^2\right\} \tag{12}$$

where N is the total number of frequencies. In this case, the number of data points is twice the number of frequencies, so that the number of degrees of freedom is $\nu = 2N - p$.

In both pulse and phase-modulation fluorometries, the value of χ_r^2 should be close to 1 for a good fit (dependent on the number of data points). Acceptable values are in the 0.8–1.2 range. Lower values indicate that the data set is too small for a meaningful fit. Higher values can arise either from a significant deviation from the theoretical model (e.g. insufficient number of exponential terms), or from artifacts (see above).

In phase-modulation fluorometry, the use of χ_r^2 deserve further comments. Values of the standard deviations, σ_Φ and σ_M, must be assigned and these values are in principle frequency dependent. At each frequency, a large number of phase shift and modulation measurements are averaged so that values of the standard deviations are easily calculated. However, it turns out generally that when such values are used in the analysis, abnormally high values of χ_r^2 are obtained, which means that such values of the standard deviations are underestimated (because of some systematic errors). Therefore, "realistic" frequency-independent values are to be assigned. The important consequence is that the value of χ_r^2 is not sufficient as a criterion of a good fit. If the standard deviations of σ_Φ and σ_M are overestimated, the value of χ_r^2 may be close to 1, and an erroneous conclusion on the goodness of the fit may be drawn. This is a common pitfall in phase-modulation fluorometry. Thus, it should be emphasized that only relative values can be used in accepting or rejecting a theoretical model. For instance, in the case of a multiexponential decay, when χ_r^2 decreases twofold or more when an exponential term is added, then addition of this term is justified.

Another useful numerical test is the "ordinary runs test" [65] in which the number of sequences of residuals with the same sign (*runs*) is counted and compared with the number expected for a set of random numbers.

Finally, the mean, standard deviation and percentage of weighted residuals within the $[-2, 2]$ interval can be calculated for SPT data. These values should be reasonably close to the predicted values of 0.0, 1.0, and 95.44%, respectively.

In addition to the numerical goodness-of-fit criteria, e.g., the value of χ_r^2 and the runs test, it is valuable to display graphical tests. Visual techniques are very informative and useful for observing trends in the data. Because time is the only observable independent variable in SPT experiments, it is useful to plot the differences between the experimental sample responses, $R(t_i)$, and the fitted ones, $R_c(t_i)$. Better even is plotting the weighted residuals defined as

$$W(t_i) = \frac{R(t_i) - R_c(t_i)}{\sigma(i)} \tag{13}$$

where $\sigma(i) = \sqrt{R(t_i)}$ for SPT data. Such a plot can be helpful in choosing the correct functional form of the model decay function $f_s(t)$. There should be no discernible trend in the plot of $W(t_i)$ versus time (or channel number i); only a random scatter of points about the line $W(t_i) = 0$. The patterns of such a plot can often reveal (1) bias, lack of fit of the proposed model [decay function $f_s(t)$], and (2) outliers, extremely large deviations between determining the experimental, $R(t_i)$, and the fitted, $R_c(t_i)$, responses in an otherwise satisfactory fit. Outliers require careful examination to find out if the reason for their particularity can be determined.

When the number of data points is large (i.e., in the SPT technique, or in phase fluorometry when using a large number of modulation frequencies), the autocorrelation function of the residuals defined as

$$C(j) = \frac{1/(N-j)\prod_{i=1}^{N-j} W(t_i)W(t_{i+j})}{(1/N)\prod_{i=1}^{N}[W(t_i)]^2} \tag{14}$$

is also a useful graphical test of the quality of the fit. $C(j)$ expresses the correlation between the weighted residuals in channel j and channel $i + j$.

Normal probability plots for the weighted residuals are sometimes useful for detecting departures from normality and outliers [65]. If the weighted residuals are normally distributed, the points should lie roughly on a straight line; otherwise, the residuals will not follow a general linear trend.

The fit is satisfactory when the weighted residuals and the autocorrelation function are randomly distributed around zero and the normal probability plot is linear. Low frequency periodicity *can be* the symptom of radiofrequency interferences (see above).

We now turn our attention to the models used in the analysis of time-resolved fluorescence data. The following considerations will apply to both pulse and phase-modulation fluorometries.

In most cases, time-resolved fluorescence data are analyzed using a sum of exponential terms. This can be indeed expected in the following situations: fluorophores in distinct forms or in distinct environments, fluorophores undergoing photoinduced processes (excited-state proton transfer, excimer formation, etc.).

When the fluorescence δ-response function of the system is not a sum of exponential terms, but a function based on a physical model, nonlinear least-squares analysis can still be performed to extract from the fluorescence decay the parameters of the model.

But what to do in the absence of a physical model? Most commonly, when a single exponential analysis fails, a fit with a sum of two exponentials is attempted. If the quality of the fit is still unsatisfactory, a third exponential term is added. In most cases, a fourth component does not improve the quality of the fit. If the quality of the fit is satisfactory with two (or three) exponentials, does it mean that the theoretical δ-pulse response of the system is a sum of two (or three) exponentials? It may simply mean that the number of fitting parameters is large enough considering the limited accuracy of the experimental data. Therefore, the recovered decay times and preexponential factors may have no physical significance. *This is the most common artifact regarding data analysis*. This artifact is not a consequence of the iterative reconvolution analysis procedure, but it results from the fact that recovery of the δ-response from fluorescence data in time or frequency domains is an ill-conditioned problem.

The quality of the experimental data is indeed of major importance. In the single-photon timing technique it has been shown [66] that with a number of 10^4 counts in the peak channel, a variety of decay laws (including distributions) can yield identical results in terms of χ_r^2, weighed residuals and autocorrelation function when subjected to a two-exponential analysis. Even when two decay times are separated by a factor of more than 2, the underlying decay can still be due to an underlying distribution of exponentials. The same considerations apply to the analysis of phase-modulation data when a relatively small number of frequencies are used. Here, the standard global analysis of related decay curves or better still the global compartmental analysis of the entire fluorescence decay surface—where the model is imposed directly on the data—can be used as an effective model-distinction tool. Collecting decays at high signal-to-noise ratios is not only a good test for the presence of systematic (non-Poissonian distributed) errors but also increases the capability to distinguish between competing models in single curve analysis. Long collection periods for individual decay traces might imply effects due the instabilities in the experimental set-up. On the other hand, a global analysis approach allows for a high model discrimination power, even at low signal-to-noise ratios.

The case of fluorescence decays with underlying distributions deserves particular attention. This is the most difficult situation in data analysis. Distributions of decay times can exist in a variety of systems: fluorophores incorporated in micelles, cyclodextrins, rigid solutions, sol–gel matrices, proteins, vesicles or membranes; fluorophores adsorbed on surfaces, or linked to surfaces; quenching of fluorophores in micellar solutions; energy transfer in assemblies of like or unlike fluorophores, etc.

If an *a priori* choice of the shape of the distribution (i.e. gaussian, sum of two gaussians, Lorentzian, sum of two Lorentzians, etc.) is made without theoretical basis, a satisfactory fit of the experimental data will only indicate that the assumed distribution is compatible with the experimental data, but it will not demonstrate that this distribution is the only one possible.

In the absence of a physical model, it is tempting to use an approach without *a priori* assumption of the shape of the distribution, such as the maximum entropy method or the exponential series method [67,68]. However, the recovered distribution can be extremely sensitive to the quality of the data. Because of the ill-conditioned nature of the distribution analysis of decay times, small systematic errors resulting from optical or electronic artifacts (see above) can cause a large change in the recovered distribution. Instability of such a distribution can indeed be observed from repeated experiments under exactly the same conditions, even when data are of excellent quality [69]. However, physically plausible results can be obtained by using an algorithm based on a combination of the Marquardt method and the smoothing technique of Phillips [69].

Considering the difficulty in the use of these non *a priori* methods, mathematical functions for the analysis of fluorescence decays with underlying distributions can be advantageously used provided that they rely on physical considerations. This is in particular the case of the stretched exponential function, defined as $\exp[-(t/\tau)^{\beta}]$ where $0 < \beta \leq 1$ (M. N. Berberan-Santos, E. N Bodunov, B. Valeur, manuscript in preparation).

CONCLUSIONS

Time-resolved fluorescence experiments require great care because of many possible pitfalls and fallacies. Many points should be carefully checked before running an experiment. When preparing a sample, attention should be paid to inner filter effects and to the possible effects of dissolved oxygen, temperature, photobleaching, autofluorescence, etc. Optical and electronic artifacts can have

many origins and it is sometimes difficult to track them. However, we have shown in the present paper that in most cases, their effects can be minimized, eliminated or corrected. Then, using appropriate strategy for data analysis, decay time measurements of only a few picoseconds are possible with excellent goodness-of-fit statistics.

ACKNOWLEDGMENTS

Prof Dr Johan Hofkens and Dr Mircea Cotlet are thanked for providing schemes of SPT set-ups which were the bases for Figures 1 and 3. Dr Nikola Basarić is thanked for supplying Figures 7, 11, and 12. N.B. is grateful to the FWO (*Fonds voor Wetenschappelijk Onderzoe—Vlaanderen*) and the University Research Fund (K.U. Leuven) for continuing support. Ms Melanie Gérard is thanked for useful discussions regarding the preparation of protein solutions.

REFERENCES

1. E. Gaviola (1926). Ein Fluorimeter: Apparat zur Messung von Fluorescenzabklingungszeiten. *Z. Physik* **42**, 853–861; E. Gaviola (1926). Die Abklingungszeiten der Fluorescenz von Farbstofflösungen. *Ann. Physik* **81**, 681–710.
2. B. Valeur (2002). *Molecular Fluorescence. Principles and Applications*, Wiley-VCH, Weinheim.
3. E. Gratton, D. M. Jameson, N. Rosato, and G. Weber (1984). Multifrequency cross-correlation phase fluorometer using synchrotron radiation. *Rev. Sci. Instrum.* **55**, 486–494.
4. S. Landgraf (2001). Application of semiconductor light sources for investigations of photochemical reactions. *Spectrochimica Acta A* **57**, 2029–2048; S. Landgraf and G. Grampp (1998). Application of laser diodes and ultrabright light emitting diodes for the determination of fluorescence lifetimes in the nano- and subnanosecond region. *J. Inform. Record.* **24**, 141–148.
5. U. K. Tirlapur and K. König (2002). Two-photon near-infrared femtosecond laser scanning confocal microscopy in plant biology. in A. Diaspro (Ed.), *Confocal and Two-Photon Microscopy. Foundations, Applications, and Advances*, Wiley-Liss, New York, pp. 449–468.
6. T. W. J. Gadella (1999). Fluorescence Lifetime Imaging Microscopy (FLIM): Instrumentation and applications. In W. T. Mason (Ed.), *Fluorescent and Luminescent Probes for Biological Activity: A practical Guide to Technology for Quantitative Real-Time Analysis*, Academic Press, San Diego, pp. 467–479.
7. D. Axelrod, E. H. Hellen, and R. M. Fulbright (1992). Total internal reflection fluorescence. In J. R. Lakowicz (Ed.), *Topics in Fluorescence Spectroscopy: Biochemical Applications*, Plenum, New York, pp. 289–343.
8. V. E. Centonze, M. Sun, A. Masuda, H. Gerritsen, and B. Herman (2003). Fluorescence resonance energy transfer imaging microscopy. In G. Marriott and I. Parker (Eds.), *Methods in Enzymology. Biophotonics, Part A*, Academic Press, Amsterdam, pp. 542–560.
9. J. R. Lakowicz (1999). *Principles of Fluorescence Spectroscopy*, Plenum, New York.
10. D. V. O'Connor and D. Phillips (1984). *Time-correlated single photon counting*, Academic Press, London.
11. N. Boens (1991). Pulse fluorometry. In W. R. G. Baeyens, D. De Keukeleire, and K. Korkidis (Eds.), *Luminescence Techniques in Chemical and Biochemical Analysis*, Marcel Dekker, New York, pp. 21–45.
12. E. Gratton, D. M. Jameson, and R. D. Hall (1984). Multifrequency phase and modulation fluorometry. *Ann. Rev. Biophys. Bioeng.* **13**, 105–124.
13. B. Valeur (2004). Pulse and phase fluorometries. An objective comparison. In M. Hof, R. Hutterer, and V. Fidler (Eds.), *Fluorescence Spectroscopy in Biology. Advanced Methods and Their Applications to Membranes, Proteins, DNA, and Cells,* Springer-Verlag, pp. 30–48.
14. E. Gratton, S. Breusegem, J. Sutin, and Q. Q. Ruan (2003). Fluorescence lifetime imaging for the two-photon microscope: Time-domain and frequency-domain methods. *J. Biomed. Optics* **8**, 381–390.
15. M. vandeVen and E. Gratton (1993). Time-resolved fluorescence lifetime imaging. In B. Herman and J. J. Lemasters (Eds.), *Optical Microscopy. Emerging Methods and Applications*, Academic Press, San Diego, pp. 373–402.
16. R. M. Clegg, O. Holub, and C. Gohlke (2003). Fluorescence lifetime-resolved imaging: Measuring lifetimes in an image. *Biophotonics A* **360**, 509–542.
17. P. J. Verveer, S. Squier, and P. I. H. Bastiaens (2001). Frequency-domain fluorescence lifetime imaging Microscopy: A window on the biochemical landscape of the cell. In A. Periasamy (Ed.), *Methods in Cellular Imaging*, Oxford University Press, Oxford, pp. 273–294.
18. R. B. Thompson and E. Gratton (1988). Phase fluorometric method for determination of standard lifetimes. *Anal. Chem.* **60**, 670–674.
19. J. N. Demas (1983). *Excited State Lifetime Measurements*, Academic Press, New York.
20. G. R. Holtom (1990). Artifacts and diagnostics in fast fluorescence measurements. In J. R. Lakowicz (Ed.), *Time-Resolved Laser Spectroscopy in Biochemistry II. SPIE Proceedings*, Vol. 1204, Los Angeles, pp. 2–12.
21. R. Kay (2004). Detecting and minimizing zinc contamination in physiological solutions. BMC *Physiol.* **4**, 4–9.
22. E. Bucci, H. Malak, C. Fronticelli, I. Gryczynski, G. Laczko, and J. R. Lakowicz (1988). Time-resolved emission spectra of hemoglobin on the picosecond time scale. *Biophys. Chem.* **32**, 187–198.
23. B. W. Van der Meer (1988). Biomembrane structure and dynamics by fluorescence. In H. J. Hilderson (Ed.), *Fluorescence Studies on Biological Membranes*. Vol. 13: *Subcellular Biochemistry*, Plenum, New York, pp. 1–53.
24. L. A. Bagatolli and E. Gratton (2001). Direct observation of lipid domains in free-standing bilayers using two-photon excitation fluorescence microscopy. *J. Fluoresc.* **11**, 141–160.
25. H. A. Clayton, Q. S. Hanley, D. J. Arndt-Jovin, V. Subramaniam, and T. M. Jovin (2002). Dynamic fluorescence anisotropy imaging microscopy in the frequency domain (rFLIM). *Biophys. J.* **83**, 1631–1649.
26. K. König (2001). Cellular response to laser radiation in fluorescence microscopes. In A. Periasamy (Ed.), *Methods in Cellular Imaging*, Oxford University Press, Oxford, pp. 236–251.
27. K. König and U. K. Tirlapur (2002). Cellular and subcellular perturbations during multiphoton microscopy. In A. Diaspro (Ed.), *Confocal and Two-Photon Microscopy. Foundations, Applications and Advances*, Wiley-Liss, New York, pp. 191–205.
28. E. M. Gill, G. M. Palmer, and N. Ramanujam (2003). Steady-state fluorescence imaging of Neoplasia. In G. Marriott and I. Parker (Eds.), *Methods in Enzymology. Biophotonics, Part B*, Academic Press, Amsterdam, pp. 452–481.
29. P. Herman, B. P. Maliwal, H. J. Lin, and J. R. Lakowicz. (2001). Frequency-domain fluorescence microscopy with the LED as a light source. *J. Microsc.* **203**, 176–181.
30. T. C. W. Brelje, M. W. Wessendorf, and R. L. Sorenson (1993). Multicolor laser scanning confocal immunofluorescence microscopy: Practical applications and limitations. In B. Matsumoto (Ed.), *Cell Biological Applications of Confocal Microscopy*, Academic Press, San Diego, pp. 97–181.

31. E. Gratton and M. J. vande Ven (1995). Laser sources for confocal microscopy. In J. B. Pawley (Ed.), *Handbook of Biological Confocal Microscopy*, Plenum, New York, pp. 69–97.
32. R. Wolleschensky, M. E. Dickinson, and S. E. Fraser (2002). Group-velocity dispersion and fiber delivery in multiphoton laser scanning microscopy. In A. Diaspro (Ed.), *Confocal and Two-Photon Microscopy. Foundations, Applications and Advances*, Wiley-Liss, New York, pp. 171–190.
33. E. Gratton and M. Limkeman (1983). A continuously variable frequency cross-correlation phase fluorometer with picosecond resolution. *Biophys. J.* **44**, 315–324.
34. D. M. Jameson, C. J. C. Croney, and P. D. J. Moens (2003). Fluorescence: Basic concepts, practical aspects, and some anecdotes. In G. Marriott and I. Parker (Eds.), *Methods in Enzymology. Biophotonics Part A*, Academic Press, Amsterdam, pp. 1–43.
35. D. Bebelaar (1986). Compensator for the time dispersion in a monochromator. *Rev. Sci. Instrum.* **57**, 1686–1687.
36. D. A. Long (1977). *Raman Spectroscopy*, McGraw-Hill, New York.
37. J. R. Lakowicz, G. Laczko, and I. Gryczynski (1986). 2-GHz frequency-domain fluorometer. *Rev. Sci. Instrum.* **57**, 2499–2506.
38. K. W. Berndt and J. R. Lakowicz (1990). 4-GHz Internal MCP-photomultiplier cross-correlation. *Rev. Sci. Instrum.* **61**, 2557–2565.
39. G. Laczko, I. Gryczynski, Z. Gryczynski, W. Wiczk, H. Malak, and J. R. Lakowicz (1990). A 10-GHz frequency-domain fluorometer. *Rev. Sci. Instrum.* **61**, 2331–2337.
40. E. Gratton and M. vandeVen (1990). A superheterodyning microwave frequency-domain fluorometer. *Biophys. J.* **57**, A378.
41. B. Barbieri, F. De Piccoli, M. vande Ven, and E. Gratton (1990). What determines the uncertainty of phase and modulation measurements in frequency domain fluorometry. In J. R. Lakowicz (Ed.), *Time-Resolved Laser Spectroscopy in Biochemistry II. SPIE Proceedings,* Vol. 1204, Los Angeles, pp. 158–170.
42. M. A. Franceschini, S. Fantini, and E. Gratton (1994). LEDs in frequency-domain spectroscopy of tissues. in *Advances in Laser and Light Spectroscopy to Diagnose Cancer and Other Diseases. SPIE Proceedings,* Vol. 2135, Los Angeles, pp. 300–306.
43. B. Barbieri, F. De Piccoli, and E. Gratton (1989). Synthesizers phase noise in frequency-domain fluorometry. *Rev. Sci. Instrum.* **60**, 3201–3206.
44. D. W. Piston, G. Marriott, T. Radivoyevich, R. M. Clegg, T. M. Jovin, and E. Gratton. (1989). Wide-band acousto-optic light modulator for frequency domain fluorometry and phosphorimetry. *Rev. Sci. Instrum.* **60**, 2596–2600
45. E. Gratton, B. Feddersen, and M. vande Ven (1990). Parallel acquisition of fluorescence decay using array detectors. In J. R. Lakowicz (Ed.), *Time-Resolved Laser Spectroscopy in Biochemistry II. SPIE Proceedings,* Vol. 1204, Los Angeles, pp. 21–25.
46. S. Canonica, J. Forrer, and U. P. Wild (1985). Improved timing resolution using small side-on photomultipliers in single photon counting. *Rev. Sci. Instrum.* **56**, 1754–1758.
47. M. P. Gordon and P. R. Selvin (2003). A microcontroller-based failsafe for single photon counting modules. *Rev. Sci. Instrum.* **74**, 1150–152.
48. M. vandeVen and E. Gratton (1993). Time-resolved fluorescence lifetime imaging. In B. Herman and J. J. Lemasters (Ed.), *Optical Microscopy. Emerging Methods and Applications*, Academic Press, San Diego, pp. 373–402.
49. T. French (1996). *The Development of Fluorescence Lifetime Imaging and an Application in Immunology,* PhD Thesis. University of Illinois at Urbana–Champaign.
50. W. Becker and A. Bergmann (2002). *Detectors for High-Speed Photon Counting*, The TCSPC Knowledge Base, Berlin. Also availabe at http//www.becker-hickl.de/pdf/spcdetect1.pdf.
51. K. Berndt (1985). Application of gain-modulated avalanche photodiodes in phase-sensitive fluorescence spectroscopy. *Optics Commun.* **56**, 30–35.
52. J. Pouget, J. Mugnier, and B. Valeur (1989). Correction of timing errors in multifrequency phase(modulation fluorometry., *J. Phys. E: Sci. Instrum.* **22**, 855–862.
53. P. Gauduchon and Ph. Wahl (1978). Pulse fluorimetry of tyrosyl peptides. *Biophys. Chem.* **8**, 87–104; R. W. Wijnaendts van Resandt, R. H. Vogel, and S. W. Provencher (1982). Double beam fluorescence lifetime spectrometer with subpicosecond resolution: Application to aqueous tryptophan. *Rev. Sci. Instrum.* **53**, 1392–1397; M. Zuker, A. G. Szabo, L. Bramall, D. T. Krajcarski, and B. Selinger (1985). Delta function convolution method (DFCM) for fluorescence decay experiments. *Rev. Sci. Instrum.* **56**, 14–22; M. Van den Zegel, N. Boens, D. Daems, and F. C. De Schryver (1986). Possibilities and limitations of the time-correlated single photon counting technique: A comparative study of correction methods for the wavelength dependence of the instrument response function. *Chem. Phys.* **101**, 311–335; N. Boens, M. Ameloot, I. Yamazaki, and F. C. De Schryver (1988). On the use and the performance of the delta function convolution method for the estimation of fluorescence decay parameters. *Chem. Phys.* **121**, 73–86.
54. N. Boens, N. Tamai, I. Yamazaki, and T. Yamazaki (1990). Picosecond single photon timing measurements with a proximity type microchannel plate photomultiplier and global analysis with reference convolution. *Photochem. Photobiol.* **52**, 911–917.
55. R. E. Imhof and D. J. S. Birch (1982). Distortion of gaussian pulses by a diffraction grating. *Optics Commun.* **42**, 83–86.
56. R. V. Krishnan, H. Saitoh, H. Terada, V. E. Centonze, and B. Herman (2003). Development of a multiphoton fluorescence lifetime imaging microscope system using a streak camera. *Rev. Sci. Instrum.* **74**, 2714–2721.
57. K. Kemnitz, L. Pfeifer, and M. R. Ainbund (1997). Detector for multichannel spectroscopy and fluorescence lifetime imaging on the picosecond timescale. *Nucl. Instrum. Methods Phys. Res, Sect. A*, **387**, 86–87.
58. F. R. Boddeke (1998). *Quantitative Fluorescence Microscopy,* Dissertation, Delft Technical University.
59. J. M. Beechem, E. James, and L. Brand (1990). Time-resolved fluorescence studies of the protein folding process: New instrumentation, analysis and experimental approaches. In J. R. Lakowicz (Ed.), *Time-Resolved Laser Spectroscopy in Biochemistry II. SPIE Proceedings,* Vol. 1204, Los Angeles, pp. 686–698.
60. J. M. Beechem (1992). Global analysis of biophysical data. In L. Brand and M. L. Johnson (Eds.), *Methods in Enzymology*, Vol. 210, Academic Press, San Diego, pp. 37–54.
61. P. J. Verveer and P. I. H. Bastiaens (2003). Evaluation of global analysis algorithms for single frequency fluorescence lifetime imaging microscopy data. *J. Microsc. Oxford*, **209**, 1–7.
62. J. M. Beechem, M. Ameloot, and L. Brand (1985). Global analysis of fluorescence decay surfaces—Excited state reactions. *Chem. Phys. Lett.* **120**, 466–472; M. Ameloot, J. M. Beechem, and L. Brand (1986). Compartmental modeling of excited state reactions. Identifiability of the rate constants from fluorescence decay surfaces. *Chem. Phys. Lett.* **129**, 211–219; M. Ameloot, N. Boens, R. Andriessen, V. Van den Bergh, and F. C. De Schryver (1991). Non a priori analysis of the fluorescence decay surfaces of excited-state processes. 1: Theory. *J. Phys. Chem.* **95**, 2041–2047; M. Ameloot, N. Boens, R. Andriessen, V. Van den Bergh, and F. C. De Schryver (1992). Compartmental analysis of fluorescence decay surfaces of excited-state processes. In L. Brand and M. L. Johnson (Eds.), *Methods in Enzymology*, Vol. 210, Academic Press, San Diego, pp. 314–340.
63. D. F. Eaton (1990). Recommended methods for fluorescence decay analysis. *Pure Appl. Chem.* **62**, 1631–1648.
64. D. Marquardt (1963). An algorithm for least squares estimation of nonlinear parameters, *J. Appl. Math.* **11**, 431–441.
65. N. Boens, M. Van den Zegel, and F. C. De Schryver (1984). Picosecond determination of the second excited singlet lifetime of xanthione in solution. *Chem. Phys. Lett.* **111**, 340–346; N. Boens,

M. Van den Zegel, and F. C. De Schryver (1984). ibid. **113**, 602.
66. D. R. James and W. R. Ware (1985). A fallacy in the interpretation of fluorescence decay parameters. *Chem. Phys. Lett.* **120**, 455–459.
67. J. C. Brochon (1994). Maximum entropy method of data analysis in time-resolved spectroscopy. In L. Brand and M. L. Johnson (Eds.), *Methods in Enzymology*, Vol. 240, Academic Press, San Diego, pp. 262–311.
68. Siemiarczuk, B. D. Wagner, and W. R. Ware (1990). Comparison of the maximum entropy and exponential series methods for the recovery of distributions of lifetimes from fluorescence lifetime data. *J. Phys. Chem.* **94**, 1661–1666.
69. Y. S. Liu and W. R. Ware (1993). Photophysics of polycyclic aromatic hydrocarbons adsorbed on silica gel surfaces. 1: Fluorescence lifetime distribution analysis. An ill-conditioned problem. *J. Phys. Chem.* **97**, 5980–5986.